ADA071327

DDC FILE COPY

FORMULATION OF ELECTROMAGNETIC PULSE
EXTERNAL INTERACTION ABOVE A LOSSY EARTH

M. I. Sancer
S. Siegel
A. D. Varvatsis

TDR, Inc.
Marina del Rey, CA 90291

Los Angeles, CA.

June 1979

Final Report

Prepared for
Director
DEFENSE NUCLEAR AGENCY
Washington, DC 20305

DDC

JUL 17 1979

A

AIR FORCE WEAPONS LABORATORY
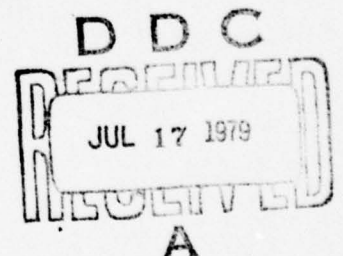Air Force Systems Command
Kirtland Air Force Base, NM 87117

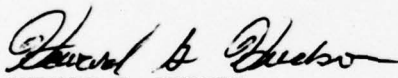79 07 17 012

Use 392 622
Los Angeles, CA.

This final report was prepared by TDR, Inc., Marina del Rev, California, under Contract F29601-77-C-0090, Job Order WDNE3206 with the Air Force Weapons Laboratory, Kirtland Air Force Base, New Mexico. Capt H. G. Hudson (ELTI) was the Laboratory Project Officer-in-Charge.

When US Government drawings, specifications, or other data are used for any purpose other than a definitely related Government procurement operation, the Government thereby incurs no responsibility nor any obligation whatsoever, and the fact that the Government may have formulated, furnished, or in any way supplied the said drawings, specifications, or other data is not to be regarded by implication or otherwise as in any manner licensing the holder or any other person or corporation or conveying any rights or permission to manufacture, use, or sell any patented invention that may in any way be related thereto.

This report has been authored by a contractor of the US Government. Accordingly, the US Government retains a nonexclusive royalty-free license to publish or reproduce the material contained herein, or allow others to do so, for the US Government purposes.
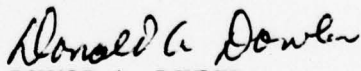
This report has been reviewed by the Office of Information (OI) and is releasable to the National Technical Information Service (NTIS). At NTIS it will be available to the general public, including foreign nationals.

This technical report has been reviewed and is approved for publication.

HOWARD G. HUDSON
Capt, USAF
Project Officer

FOR THE COMMANDER

J. PHILIP CASTILLO
Chief, Technology Branch

DONALD A. DOWLER
Col, USAF
Chief, Electromagnetics Division

REPORT DOCUMENTATION PAGE		READ INSTRUCTIONS BEFORE COMPLETING FORM
1. REPORT NUMBER AFWL-TR-78-173	2. GOVT ACCESSION NO.	3. RECIPIENT'S CATALOG NUMBER
4. TITLE *(and Subtitle)* FORMULATION OF ELECTROMAGNETIC PULSE EXTERNAL INTERACTION ABOVE A LOSSY EARTH		5. TYPE OF REPORT & PERIOD COVERED Final Report
		6. PERFORMING ORG. REPORT NUMBER
7. AUTHOR(s) M. I. Sancer A. D. Varvatsis S. Siegel		8. CONTRACT OR GRANT NUMBER(s) F29601-77-C-0090
9. PERFORMING ORGANIZATION NAME AND ADDRESS TDR, Inc. Marina del Rey, CA 90291		10. PROGRAM ELEMENT, PROJECT, TASK AREA & WORK UNIT NUMBERS 62704H WDNE3206
11. CONTROLLING OFFICE NAME AND ADDRESS Director Defense Nuclear Agency Washington, D.C. 20305		12. REPORT DATE June 1979
		13. NUMBER OF PAGES 60
14. MONITORING AGENCY NAME & ADDRESS(if different from Controlling Office) Air Force Weapons Laboratory (ELTI) Kirtland Air Force Base, NM 87117		15. SECURITY CLASS. (of this report) UNCLASSIFIED
		15a. DECLASSIFICATION/DOWNGRADING SCHEDULE

16. DISTRIBUTION STATEMENT (of this Report)

Approved for public release; distribution unlimited.

17. DISTRIBUTION STATEMENT (of the abstract entered in Block 20, if different from Report)

18. SUPPLEMENTARY NOTES

This research was sponsored by the Defense Nuclear Agency under Subtask R99QNXEB200, Work Unit 71, Title: Hardness Surveillance.

19. KEY WORDS (Continue on reverse side if necessary and identify by block number)

Electromagnetic Pulse Scattering
Magnetic Field Integral Equation
Ineraction Above a Perfectly Conducting Ground
Interaction Above a Lossy Earth
Patch Zoning Method
Free Field Interaction

20. ABSTRACT (Continue on reverse side if necessary and identify by block number)

Both the electric field integrodifferential equation (EFIDE) and the magnetic field integral equation (MFIE) for the determination of the surface current density induced on a perfectly conducting object above a lossy earth are derived. The resulting equations are then decomposed so that the source terms and operators are represented as the sums of three terms. For either the EFIDE or the MFIE, equating one of the source terms with one of the operator terms describes free field interaction, equating the sum of two of the source terms

DD FORM 1473 EDITION OF 1 NOV 65 IS OBSOLETE
1 JAN 73

with the sum of two of the operator terms describes interaction above a perfectly conducting ground, and equating the sum of all three source and operator terms describes interaction above a lossy earth. In this decomposition, the calculation of any of the source terms is algebraic for plane wave incidence; however, the calculation of the third operator term that changes a perfectly conducting earth to a lossy earth requires the evaluation of Sommerfeld integrals. We assure the computational tractability of these Sommerfeld integrals by presenting them in well-studied forms.

Finally, we demonstrate the capability of patch zoning the MFIE by presenting a comparison of numerical computations with experimental data. Utilizing the first term in the described decomposition, calculations for the induced surface current density are compared to the density measured on exactly the same aircraft model. Utilizing the first two terms, we compared calculated and measured current densities induced on a finite perfectly conducting cylinder above and parallel to a perfectly conducting ground. The computer code which contains these capabilities is referred to as NEC-ZA.

CONTENTS

ILLUSTRATIONS

SECTION I

INTRODUCTION

Two separate but related efforts are described in this report. The first and more significant effort is a demonstration of the capability of the patch zoning method for numerically solving the magnetic field integral equation (MFIE). This is accomplished by comparing experimental data with numerical computations of the current density induced on metallic structures. The most immediate impact of this capability is its effect on determining the potential and limitations of experimental procedures.

The structures that were treated numerically and experimentally are an aircraft model in free space and a metallic cylinder of finite length in free space and also above and parallel to a metallic ground plane. The experiments were performed at the University of Michigan by Valdis Liepa and his associates under contract to the Air Force Weapons Laboratory.

The secondary effort is a derivation of the electric field integrodifferential equation (EFIDE) and the MFIE for electromagnetic pulse external interaction with perfectly conducting bodies above a finitely conducting half-space. The relationship between the two efforts is that the equations are represented in such a manner that the computational results, which are compared with experimental data, are readily seen to correspond to the numerical treatment of special cases of the MFIE finitely conducting ground equations.

The derivation of the EFIDE and the MFIE, which include lossy earth effects, utilizes the explicit representations of

5

Green's dyadics given by Tai (ref. 1) after appropriately
accounting for missing terms (ref. 2). The results obtained
by the straightforward use of Tai's dyadic representations
contain infinite sums of infinite integrals. We introduce a
procedure that primarily consists of a coordinate change that
reduces these sums to finite sums of well studied Sommerfeld
integrals. The reduction of the infinite sums to finite sums
was not unexpected since we could have obtained the same
results by appropriately combining vertical and horizontal
dipole solutions.

    To enhance the utility of our equations, we change Tai's
notation to that of Baños (ref. 3) after the infinite sum
reductions. We do this for two reasons. First, Baños presents
a detailed theoretical investigation of the resulting Sommer-
feld integrals.   The other reason is that the work of Lytle
and Lager (refs. 4, 5) uses Baños notation and it contains com-
puter codes for the evaluation of the Sommerfeld integrals.
The recent work of Haddad and Chang (ref. 6) also contains both
theoretical and numerical work related to the evaluation of
the Sommerfeld integrals.

SECTION II

PRESENTATION OF UNSIMPLIFIED REPRESENTATIONS
FOR $\underline{E}(\underline{r})$ AND $\underline{H}(\underline{r})$

For the purpose of this analysis it is convenient to divide our volume of interest into two regions (fig. 1), V_F and V_C. V_F is the volume bounded by the surface of the object, S, the interface surface, S_B, and the upper hemisphere at infinity, $S_{F\infty}$. V_F includes the volume V_J over which the source $\underline{J}(\underline{r})$ is defined. V_C is the semi-infinite volume bounded by S_B and the lower hemisphere at infinity. The equations satisfied in each region are

$$\nabla \times \underline{E}_1(\underline{r}) = i\omega\mu_o \underline{H}_1(\underline{r}) \qquad \underline{r} \in V_F \qquad (1)$$

$$\nabla \times \underline{H}_1(\underline{r}) = -i\omega\epsilon_o \underline{E}_1(\underline{r}) + \underline{J}(\underline{r}) \qquad \underline{r} \in V_F \qquad (2)$$

and $\underline{J}(\underline{r}) = 0$ unless $\underline{r} \in V_J$. The equations in V_C are

$$\nabla \times \underline{E}_2(\underline{r}) = i\omega\mu_o \underline{H}_2(\underline{r}) \qquad \underline{r} \in V_C \qquad (3)$$

$$\nabla \times \underline{H}_2(\underline{r}) = -i\omega\epsilon \underline{E}_2(r) \qquad \underline{r} \in V_C \qquad (4)$$

where ϵ is a complex function of ω [i.e., $\epsilon = \epsilon_R(\omega) + i\epsilon_I(\omega)$] to account for the fact that the half space V_C is lossy and frequency dispersive. Combining equations 1 and 2 we obtain

$$L_F \underline{E}_1(\underline{r}) = i\omega\mu_o \underline{J}(\underline{r}) \qquad (5)$$

where

$$L_F = \nabla \times \nabla \times - k_o^2 \qquad (6)$$

7
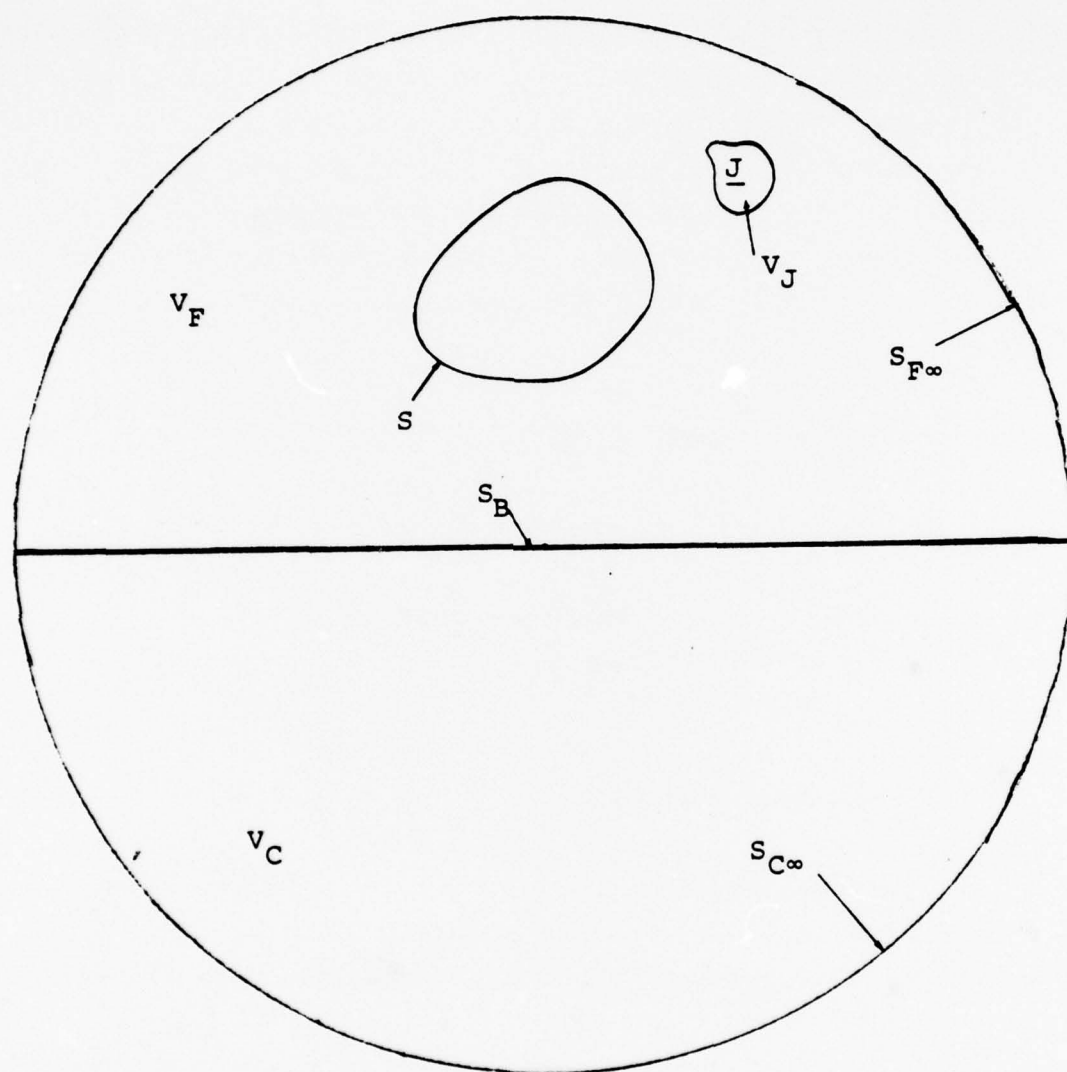
Figure 1. Geometry for Electromagnetic Scattering
from a Perfectly Conducting Body Situated Above
a Finitely Conducting Half Space.

8

and

$$k_o^2 = \omega^2 \mu_o \varepsilon_o.$$

Similarly combining equations 3 and 4 we obtain

$$L_C \underline{E}_2(\underline{r}) = 0 \tag{7}$$

where

$$L_C = \nabla \times \nabla \times -k^2 \tag{8}$$

and

$$k^2 = \omega^2 \mu_o \varepsilon. \tag{9}$$

Next we introduce the Green's dyadics that satisfy the equations

$$L_F \overline{\overline{G}}_1(\underline{r},\underline{r}_o) = \overline{\overline{I}} \, \delta(\underline{r} - \underline{r}_o) \qquad \underline{r},\underline{r}_o \, \epsilon \, V_F \tag{10}$$

and

$$L_C \overline{\overline{G}}_2(\underline{r},\underline{r}_o) = \overline{\overline{I}} \, \delta(\underline{r} - \underline{r}_o) \qquad \begin{matrix} \underline{r} \, \epsilon \, V_C \\ \underline{r}_o \, \epsilon \, V_F \end{matrix} \tag{11}$$

Next we use the dyadic identity for an arbitrary vector $\underline{a}$ and dyadic $\overline{\overline{A}}$ found in reference 7. That is

9

$$\int_V \left\{ \left(\nabla \times (\nabla \times \underline{a}) \right) \cdot \overline{\overline{A}} - \underline{a} \cdot \left(\nabla \times (\nabla \times \overline{\overline{A}}) \right) \right\} \, dV$$

$$= \int_S \left\{ (\hat{n} \times \underline{a}) \cdot (\nabla \times \overline{\overline{A}}) + \left(\hat{n} \times (\nabla \times \underline{a}) \right) \cdot \overline{\overline{A}} \right\} dS \qquad (12)$$

where V is an arbitrary volume bounded by the closed surface S which has an outward normal $\hat{n}$. By adding and subtracting either $-k_o^2 \underline{a} \cdot \overline{\overline{A}}$ or $-k^2 \underline{a} \cdot \overline{\overline{A}}$ the identity (eq. 12) can be expressed as either of the following two identities.

$$\int_S \left\{ (L_F \underline{a}) \cdot \overline{\overline{A}} - \underline{a} \cdot (L_F \overline{\overline{A}}) \right\} \, dV$$

$$= \int_S \left\{ (\hat{n} \times \underline{a}) \cdot (\nabla \times \overline{\overline{A}}) + \left(\hat{n} \times (\nabla \times \underline{a}) \right) \cdot \overline{\overline{A}} \right\} dS \qquad (13)$$

or

$$\int_V \left\{ (L_C \underline{a}) \cdot \overline{\overline{A}} - \underline{a} \cdot (L_C \overline{\overline{A}}) \right\} \, dV$$

$$= \int_S \left\{ (\hat{n} \times \underline{a}) \cdot (\nabla \times \overline{\overline{A}}) + \left(\hat{n} \times (\nabla \times \underline{a}) \right) \cdot \overline{\overline{A}} \right\} dS. \qquad (14)$$

We now employ equation 13 where $\underline{a} = \underline{E}_1(\underline{r})$ and $\overline{\overline{A}} = \overline{\overline{G}}_1(\underline{r}, \underline{r}_o)$ and $V = V_F$. Using equations 1, 5 and 10 we obtain

$$\underline{E}(\underline{r}_o) = \underline{E}_T(\underline{r}_o) + \underline{I}_S + \underline{I}_{SB1} + \underline{I}_{SF\infty} \qquad (15)$$

10

where

$$\underline{E}_T(\underline{r}_o) = \int_{V_J} (i\omega\mu_o)\left(\underline{J}(\underline{r}) \cdot \overline{\overline{G}}_1(\underline{r},\underline{r}_o)\right) \, dV \tag{16}$$

$$\underline{I}_S = i\omega\mu_o \int_S \left(\hat{n}_s(\underline{r}) \times \underline{H}(\underline{r})\right) \cdot \overline{\overline{G}}_1(\underline{r},\underline{r}_o) \, dS \tag{17}$$

$$\underline{I}_{SF\infty} = -\int_{SF\infty} \left\{ \left(\hat{n}_\infty(\underline{r}) \times \underline{E}_1(\underline{r})\right) \cdot \left(\nabla \times \overline{\overline{G}}_1(\underline{r},\underline{r}_o)\right) \right.$$

$$\left. + i\omega\mu_o\left(\hat{n}_\infty(\underline{r}) \times \underline{H}_1(\underline{r})\right) \cdot \overline{\overline{G}}_1(\underline{r},\underline{r}_o) \right\} \, dS \tag{18}$$

$$\underline{I}_{SB1} = -\int_{S_B} \left\{ \left(\hat{n}_{B1}(\underline{r}) \times \underline{E}_1(\underline{r})\right) \cdot \left(\nabla \times \overline{\overline{G}}_1(\underline{r},\underline{r}_o)\right) \right.$$

$$\left. + i\omega\mu_o\left(\hat{n}_{B1}(\underline{r}) \times \underline{H}_1(\underline{r})\right) \cdot \overline{\overline{G}}_1(\underline{r},\underline{r}_o) \right\} \, dS \tag{19}$$

and $\hat{n}_s(\underline{r})$ is the outward normal to S. Similarly, employing equation 14 for $\underline{a} = \underline{E}_2(\underline{r})$, $\overline{\overline{A}} = \overline{\overline{G}}_2(\underline{r},\underline{r}_o)$, $V = V_C$ and using equations 3, 7 and 11 we obtain

$$\int_{V_C} \left(\underline{E}_2(\underline{r}) \cdot \left(\overline{\overline{I}} \, \delta(\underline{r} - \underline{r}_o)\right)\right) \, dV = \underline{I}_{SB2} + \underline{I}_{SC\infty} \tag{20}$$

where

$$\underline{I}_{SB2} = -\int_{S_B} \left\{ \left(\hat{n}_{B2}(\underline{r}) \times \underline{E}_2(\underline{r})\right) \cdot \left(\nabla \times \overline{\overline{G}}_2(\underline{r},\underline{r}_o)\right) \right.$$

$$\left. + i\omega\mu_o\left(\hat{n}_{B2} \times \underline{H}_2(\underline{r})\right) \cdot \overline{\overline{G}}_2(\underline{r},\underline{r}_o) \right\} \, dS \tag{21}$$

11

$$I_{SC\infty} = -\int\limits_{SC\infty} \left\{ \left(\hat{n}_\infty \times \underline{E}_2(\underline{r})\right) \cdot \left(\nabla \times \overline{\overline{G}}_2(\underline{r},\underline{r}_o)\right) \right.$$

$$\left. + i\omega\mu_o \left(\hat{n}_\infty \times \underline{H}_2(\underline{r})\right) \cdot \overline{\overline{G}}_2(\underline{r},\underline{r}_o) \right\} dS. \tag{22}$$

We now simplify equations 15 and 20 by employing the boundary conditions satisfied by the fields and the Green's dyadics. First we note that $\underline{I}_{SF\infty} = 0$ as a result of the radiation condition and $\underline{I}_{SC\infty} = 0$ as a result of the exponential decay due to losses (the radiation condition would be sufficient if ε were purely real). Next we note that the volume integral in equation 20 is zero because the integration is over V_C and according to equation 11, $\underline{r}_o \in V_F$. Combining these results we can write equations 15 and 20 as

$$\underline{E}(\underline{r}_o) = \underline{E}_T(\underline{r}_o) + i\omega\mu_o \int\limits_S \underline{J}_s(\underline{r}) \cdot \overline{\overline{G}}_1(\underline{r},\underline{r}_o)\ dS + \underline{I}_{SB1} \tag{23}$$

and

$$\underline{I}_{SB2} = 0 \tag{24}$$

where we have used equation 17 and the definition

$$\underline{J}_s(\underline{r}) = \hat{n}_s(\underline{r}) \times \underline{H}(\underline{r}). \tag{25}$$

We now use the fact that $\hat{n} \times \underline{E}$ and $\hat{n} \times \underline{H}$ are continuous across the interface and that $\overline{\overline{G}}_1$ and $\overline{\overline{G}}_2$ are chosen with this fact in mind in order that $\underline{I}_{SB1} = \underline{I}_{SB2}$ which according to equation 24 equals zero in order to write equation 23 as

$$\underline{E}(\underline{r}_o) = \underline{E}_T(\underline{r}_o) + i\omega\mu_o \int\limits_S \underline{J}_s(\underline{r}) \cdot \overline{\overline{G}}_1(\underline{r},\underline{r}_o)\ dS. \tag{26}$$

12

We now return to equation 17 which combined with the information contained in equation 26 enables the interpretation (and evaluation for plane wave excitation) of $\underline{E}_T(\underline{r}_o)$ without explicitly performing the indicated integral over V_J. From equation 16 we see that $\underline{E}_T(\underline{r}_o)$ is independent of the surface S. From equation 26 we see that by imagining S to vanish, $\underline{E}_T(\underline{r}_o)$ can be interpreted as the total field, incident plus scattered, due to the lossy half-space with S absent. For an incident plane wave, $\underline{E}_T(\underline{r}_o)$ would be simply expressed (algebraically) in terms of the Fresnel reflection coefficients.

We now rewrite equation 26 with the following change variables to conform to standard notation, i.e., $\underline{r}_o$ is now denoted as $\underline{r}$ and $\underline{r}$ is now denoted as $\underline{r}'$. The resulting equation is

$$\underline{E}(\underline{r}) = \underline{E}_T(\underline{r}) + i\omega\mu_o \int_S \underline{J}_s(\underline{r}') \cdot \overline{\overline{G}}_1(\underline{r}',\underline{r}) \, dS' \tag{27}$$

which can be rewritten as

$$\underline{E}(\underline{r}) = \underline{E}_T(\underline{r}) + i\omega\mu_o \int_S \overset{\sim}{\overline{\overline{G}}}_1(\underline{r}',\underline{r}) \cdot \underline{J}_s(\underline{r}') \, dS' \tag{28}$$

where $\sim$ denotes transpose. We now use the fact that

$$\overset{\sim}{\overline{\overline{G}}}_1(\underline{r}',\underline{r}) = \overline{\overline{G}}_3^{(11)}(\underline{r},\underline{r}') \tag{29}$$

where $\overline{\overline{G}}_3^{(11)}(\underline{r},\underline{r}')$ is the notation used by Tai (ref. 1) and has exactly the same meaning implied in that book. Combining equations 28 and 29 we have

$$\underline{E}(\underline{r}) = \underline{E}_T(\underline{r}) + i\omega\mu_o \int_S \overline{\overline{G}}_3^{(11)}(\underline{r},\underline{r}') \cdot \underline{J}_s(\underline{r}') \, dS'. \tag{30}$$

13

Up to this point, all of the work presented has been tutorial; now we make our first significant point. As pointed out by Tai (ref. 2), the dyadics presented in his book lack necessary terms. His method of correcting these dyadics leads to expressions that do not explicitly exhibit the best form for subsequent numerical treatment. For the lossy half-space dyadic (and others as well) we can express the dyadic as the sum of two terms

$$\bar{\bar{G}}_3^{(11)}(\underline{r},\underline{r}') = \bar{\bar{G}}_o(\underline{r},\underline{r}') + \bar{\bar{G}}_{3s}^{(11)}(\underline{r},\underline{r}') \tag{31}$$

and the omitted terms were omitted only from $\bar{\bar{G}}_o(\underline{r},\underline{r}')$, the free space Green's dyadic. By correcting $\bar{\bar{G}}_o(\underline{r},\underline{r}')$ by supplying the missing $\underline{L}$ related dyadic terms (or equivalently the missing δ-function term) we would end up with a representation for $\bar{\bar{G}}_o(\underline{r},\underline{r}')$ that would not be as useful for numerical purposes as the standard representation that does not contain the $\underline{L}$, $\underline{M}$, and $\underline{N}$ related dyadics. The following two observations are the basis of this claim:

1) The expanded version of $\bar{\bar{G}}_o(\underline{r},\underline{r}')$ will always contain two different representations that require separate numerical treatment, depending on whether one of the spatial observation point coordinates is larger or smaller than the corresponding integration point coordinate.

2) The derivation of the integral equation in the magnetic field case, or the integrodifferential equation in the electric field case, requires that the limit be properly treated as the observation point approaches the integration point on the surface S. By expressing $\bar{\bar{G}}_o(\underline{r},\underline{r}')$ in the standard closed form, we can make use of existing analysis to treat this limit. With this as background we have the following representations:

$$\bar{\bar{G}}_o(\underline{r},\underline{r}') = \left(\bar{\bar{I}} + \frac{1}{k_o^2}\nabla\nabla\right)g \tag{32a}$$

14

where

$$g = \left(4\pi |\underline{r} - \underline{r}'|\right)^{-1} \exp\left(ik_o |\underline{r} - \underline{r}'|\right) \qquad (32b)$$

and

$$\bar{\bar{G}}_{3s}^{(11)}(\underline{r},\underline{r}') = \frac{i}{4\pi} \int_0^\infty \frac{d\lambda}{\lambda h_1} \sum_{n=0}^\infty \sum_{\alpha=e,o} (2 - \delta_{no}) \left\{ a\underline{M}_{\alpha n\lambda}(h_1)\underline{M}'_{\alpha n\lambda}(h_1) \right.$$
$$\left. + b\underline{N}_{\alpha n\lambda}(h_1)\underline{N}'_{\alpha n\lambda}(h_1) \right\} \qquad (33a)$$

where

$$\underline{M}_{\substack{e\\o}n\lambda}(h_1) = \nabla \times \left[J_n(\lambda r) \frac{\cos}{\sin} n\phi \ e^{ih_1 z} \ \hat{z} \right] \qquad (33b)$$

$$\underline{N}_{\substack{e\\o}n\lambda}(h_1) = \frac{1}{k_o} \nabla \times \underline{M}_{\substack{e\\o}n\lambda}(h_1) \qquad (33c)$$

$$a = \frac{h_1 - h_2}{h_1 + h_2} \qquad (33d)$$

$$b = \frac{k_2^2 h_1 - k_o^2 h_2}{k_2^2 h_1 + k_o^2 h_2} \qquad (33e)$$

$$k_o^2 = \omega^2 \mu_o \varepsilon_o \qquad (33f)$$

$$k_2^2 = \omega^2 \mu_o \varepsilon; \ \varepsilon \text{ is the complex permittivity} \atop \text{of the lossy half-space} \qquad (33g)$$

$$h_1 = \left(k_o^2 - \lambda^2\right)^{1/2} \qquad (33h)$$

$$h_2 = \left(k_2^2 - \lambda^2\right)^{1/2} \qquad (33i)$$

15

and δ_{no} is the Kronecker delta function. Implied, by the explicit relationships presented in equation 33, is a coordinate system having its origin at the interface between the semi-infinite lossless half-space and the semi-infinite lossy half-space. The usual cylindrical coordinate system is employed with z being measured as positive as the distance from the interface is increased into the lossless medium. In summary, equations 28 through 33 present an explicit representation for the electric field, $\underline{E}(\underline{r})$, off the surface S once $\underline{J}_S(\underline{r})$ has been determined. A discussion concerning the determination of an appropriate equation having $\underline{J}_S(\underline{r})$ as its solution will be given in subsequent sections. The equations that present an explicit representation for $\underline{H}(\underline{r})$ off the surface S, once $\underline{J}_S(\underline{r})$ is determined, are arrived at by taking the curl of equation 28 and employing equation 1. The resulting representation is

$$\underline{H}(\underline{r}) = \underline{H}_T(\underline{r}) + \int_S \overline{\overline{K}}(\underline{r},\underline{r}') \cdot \underline{J}_S(\underline{r}') \, dS' \tag{34}$$

where

$$\overline{\overline{K}}(\underline{r},\underline{r}') = \nabla \times \overline{\overline{G}}_3^{(11)}(\underline{r},\underline{r}') \tag{35}$$

and employing the same arguments that led to the interpretation of $\underline{E}_T(r)$ without the explicit evaluation of equation 16, we can interpret

$$\underline{H}_T(\underline{r}) = \frac{1}{i\omega\mu_o} \nabla \times \underline{E}_T(\underline{r}) \tag{36}$$

as the total magnetic field $\left(\underline{H}_T(\underline{r})\right)$, incident plus scattered, due to the lossy half space with S absent. For an incident plane wave, $\underline{H}_T(\underline{r})$ would simply be algebraically expressed in terms of Fresnel reflection coefficients.

We now simplify equation 35, to a limited extent, by straight-forward substitution. In the next section we will simplify it

16

a great deal more and discuss the numerical benefits of the form we ultimately obtain. First we write

$$\bar{\bar{K}}(\underline{r},\underline{r}') = \bar{\bar{K}}_o(\underline{r},\underline{r}') + \bar{\bar{K}}_s(\underline{r},\underline{r}') \tag{37}$$

where

$$\bar{\bar{K}}_o = \nabla \times \bar{\bar{G}}_o(\underline{r},\underline{r}') = \nabla g \times \bar{\bar{I}} \tag{38}$$

and

$$\bar{\bar{K}}_s = \nabla \times \bar{\bar{G}}_{3s}^{(11)}(\underline{r},\underline{r}') \tag{39}$$

with $\bar{\bar{G}}_{3s}^{(11)}(\underline{r},\underline{r}')$ given by equation 33. Equation 39 can be simplified by employing equation 33c and the relationship

$$\nabla \times \underline{N}e_{on\lambda}(h_1) = k_o \underline{M}e_{on\lambda}(h_1). \tag{40}$$

The expression obtained is

$$\bar{\bar{K}}_s(\underline{r},\underline{r}') = \frac{ik_o}{4\pi} \int_o^\infty \frac{d\lambda}{\lambda h_1} \sum_{n=0}^\infty \sum_{\alpha=e,o} (2 - \delta_{no}) \left\{ a\underline{N}_{\alpha n\lambda}(h_1)\underline{M}'_{\alpha n\lambda}(h_1) \right.$$

$$\left. + b\underline{M}_{\alpha n\lambda}(h_1)\underline{N}'_{\alpha n\lambda}(h_1) \right\}. \tag{41}$$

The resulting expression for $\underline{H}(\underline{r})$ is

$$\underline{H}(\underline{r}) = \underline{H}_T(\underline{r}) + \int_S \left(\nabla g \times \underline{J}_s(\underline{r}')\right) dS'$$

$$+ \int_S \left(\bar{\bar{K}}_s(\underline{r},\underline{r}') \cdot \underline{J}_s(\underline{r}')\right) dS' . \tag{42}$$

17

SECTION III

PRESENTATION OF THE ELECTRIC FIELD INTEGRODIFFERENTIAL EQUATION (EFIDE) AND THE MAGNETIC FIELD INTEGRAL EQUATION (MFIE) IN UNSIMPLIFIED FORM

The representation for the electric field off the surface is given by combining equations 30, 31, and 32 to obtain

$$\underline{E}(\underline{r}) = \underline{E}_T(\underline{r}) + i\omega\mu_o \left\{ \int_S g\left(|\underline{r} - \underline{r}'|\right) \underline{J}_s(\underline{r}') \, dS' \right.$$

$$\left. + \frac{1}{k_o^2} \int_S \nabla\nabla g \cdot \underline{J}_s(\underline{r}') \, dS' + \int_S \bar{\bar{G}}_{3s}^{(11)}(\underline{r},\underline{r}') \cdot \underline{J}_s(\underline{r}') \, dS' \right\} . \tag{43}$$

We take the cross product of both sides of equation 43 with $\hat{n}(\underline{r})$ where $\underline{r}$ is the point on S approached by the r in equation 43 which was a point off the surface in that equation. We also consider the behavior of the second integral in equation 43 as the volume observation point approaches the surface. (The behavior of the other two integrals requires no special treatment.) The behavior of this limit was treated in reference 8 and we can directly use those results by employing representation 31. Finally, by following the described steps and employing the boundary condition

$$\hat{n}(\underline{r}) \times \underline{E}(\underline{r}) = 0 \qquad \underline{r} \in S \tag{44}$$

we obtain our unsimplified EFIDE

$$-\hat{n}(\underline{r}) \times \underline{E}_T(\underline{r}) = i\omega\mu_o \ \hat{n}(\underline{r}) \times \left\{ \iint_S g\left(|\underline{r} - \underline{r}'|\right) \ \underline{J}_s(\underline{r}') \ dS' \right.$$

$$\left. + L\underline{J}_s(\underline{r}') + \int_S G_{3s}^{(11)}(\underline{r},\underline{r}') \cdot \underline{J}_s(\underline{r}') \ dS' \right\} \tag{45}$$

where equivalent representations of L are

$$k_o^2 \ L\underline{J}_s(\underline{r}') = \nabla\nabla \cdot \int_S g\left(|\underline{r} - \underline{r}'|\right) \underline{J}_s(\underline{r}') \ dS' \tag{46a}$$

$$= \nabla \int g\left(|\underline{r} - \underline{r}'|\right) \nabla' \cdot \underline{J}_s(\underline{r}') \ dS' \tag{46b}$$

$$= \fint \nabla g\left(|\underline{r} - \underline{r}'|\right) \nabla' \cdot \underline{J}_s(\underline{r}') \ dS' \tag{46c}$$

$$= \int g|\underline{r} - \underline{r}'| \ \nabla'\nabla' \cdot \underline{J}_s(\underline{r}') \ dS' \tag{46d}$$

$$= \nabla \fint \nabla g\left(|\underline{r} - \underline{r}'|\right) \cdot \underline{J}_s(\underline{r}') \ dS' \tag{46e}$$

and the principal value sign is only employed when it is required.

The MFIE is obtained by taking the cross of both sides of equation 42 with the $\hat{n}(\underline{r})$ just described. We also consider the behavior of the first integral in equation 42 as the volume observation point approaches the surface. This limit is precisely the one treated in the free space MFIE and its result is known. The second integral in equation 42 requires no special treatment as the volume observation point approaches the surface observation point. Again, this is a major benefit of the Green's dyadic representation 31. The

19

MFIE resulting from taking the described cross product and limit is

$$f(\Omega) \ \underline{J}(\underline{r}) = \hat{n}(\underline{r}) \times \underline{H}_T(\underline{r}) + \int_S \left\{ \hat{n}(\underline{r}) \times \left(\nabla g \times \underline{J}(\underline{r}') \right) \right\} \, dS'$$

$$+ \int_S \left\{ \hat{n}(\underline{r}) \times \bar{\bar{K}}_s(\underline{r}, \underline{r}') \cdot \underline{J}(\underline{r}') \right\} \, dS' \qquad (47)$$

where we have used the definition (25) and dropped the subscripts on $\underline{J}(\underline{r})$. The $f(\Omega)$ comes from the limiting process associated with the first integral in equation 42 and is

$$f(\Omega) = 1 - \Omega/4\pi \qquad (48)$$

where Ω is the solid angle subtended by the surface S at $\underline{r}$. If we don't choose $\underline{r}$ at a discontinuity in curvature, then $\Omega = 2\pi$ and $f(\Omega)$ assumes the value 1/2 which is usually seen in the magnetic field integral equation.

SECTION IV

DERIVATION OF THE TRACTABLE FORMS FOR THE EFIDE AND THE MFIE

An examination of the EFIDE presented in equation 45 and the MFIE in equation 47 reveals that the subsequent numerical treatment of either of these equations requires the treatment of an infinite sum of infinite integrals. This is the case because equation 45 contains $\overline{\overline{G}}_{3s}^{(11)}(\underline{r}, \underline{r}')$ defined by equation 33 and equation 47 contains $\overline{\overline{K}}_s(\underline{r}, \underline{r}')$ defined by equation 41. The objective of the work presented in this section is to derive new exact representations for $\overline{\overline{G}}_{3s}^{(11)}(\underline{r}, \underline{r}')$ and $\overline{\overline{K}}_s(\underline{r}, \underline{r}')$ as finite sums of demonstrably convergent integrals. These new representations when substituted into equations 45 and 47 constitute the tractable forms for the EFIDE and the MFIE.

The method of obtaining the simplified forms relies on the interpretation of the $\underline{r}$ and $\underline{r}'$ that appear in $\overline{\overline{G}}_3^{(11)}(\underline{r}, \underline{r}')$ presented for the first time in equation 29. After the change in variables and transposition, then $\overline{\overline{G}}_3^{(11)}(\underline{r}, \underline{r}')$ satisfies the equation

$$\nabla \times \nabla \times \overline{\overline{G}}_3^{(11)}(\underline{r}, \underline{r}') - k_o^2 \, \overline{\overline{G}}_3^{(11)}(\underline{r}, \underline{r}') = \overline{\overline{I}} \delta(\underline{r} - \underline{r}') \qquad (49)$$

where the derivatives associated with the curl operator are with respect to the $\underline{r}$ variation, and the boundary conditions at infinity and at the interface are applied to $\underline{r}$ approaching infinity and $\underline{r}$ on the interface. This interpretation means that $\underline{r}'$ is not required to vary for representations 33 and 41 to be valid. Even though $\underline{r}'$ is not required to be a variable for those representations, the application of those representations, for example equations 45 and 47, do require that $\underline{r}'$ be a variable point that has no particular restrictions. We use these facts in the following manner. First consider that we have a fixed coordinate system in which $\underline{r}$ and $\underline{r}'$ are

radius vectors to the observation point and source point respectively. Next, consider that we have another coordinate system in which the radius vector to the observation point is denoted as $\underline{r}_D$ and the radius vector to the source point is denoted $\underline{r}_D'$. The subscript D is employed to indicate that the second coordinate system is oriented in a special manner with respect to the delta function that appears in equation 49. The relationship between these two coordinate systems will now be described with the aid of the following figure.
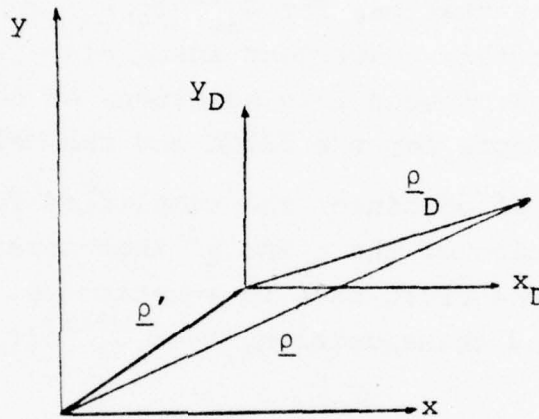
Figure 2. Coordinate Systems

The origin for both coordinate systems is on the interface and z and z_D are measured positive as the distance normal to interface increases into the lossless medium. The reason that the subscript D is employed can now be explicitly stated as

$$\underline{r}_D' = z' \, \hat{a}_z. \tag{50}$$

i.e., D refers to the fact that in this coordinate system, the origin lies directly under the delta function source. The reason for introducing the D coordinate system is that

22

r_D and r_D' satisfy the described requirements for equations 33 and 41 to be a valid representation in that system. Upon using this special representation for r_D' we will find that the infinite sums in equations 33 and 41 reduce to finite sums. After obtaining the simplified representations for $\bar{\bar{G}}_{3s}^{(11)}(r_D, r_D')$ and $\bar{\bar{K}}_s(r_D, r_D')$ we are not in a position to use the representations in equations 45 and 47 because r_D' is not free to vary in the D coordinate system. We obtain our simplified representations that can be used in equations 45 and 47 by explicitly performing the substitutions implied by the following equations

$$\bar{\bar{G}}_{3s}^{(11)}(\underline{r}, \underline{r}') = \bar{\bar{G}}_{3s}^{(11)}\big(\underline{r}_D(\underline{r}, \underline{r}'),\ \underline{r}_D'(\underline{r}, \underline{r}')\big) \tag{51}$$

$$\bar{\bar{K}}_s(\underline{r}, \underline{r}') = \bar{\bar{K}}_s\big(\underline{r}_D(\underline{r}, \underline{r}'),\ \underline{r}_D'(\underline{r}, \underline{r}')\big) \tag{52}$$

with the relationship between the coordinates (see fig. 2) given according to

$$\underline{\rho}_D = \underline{\rho} - \underline{\rho}' \tag{53}$$

$$z_D = z \tag{54}$$

$$z_D' = z' \ . \tag{55}$$

We will now present explicit results obtained by following the described procedure. First we note that for r_D' given by equation 50, the only $\underline{M}'_{\alpha n \lambda}(h_1, \underline{r}_D')$ and $\underline{N}'_{\alpha n \lambda}(h_1, \underline{r}_D')$ that are nonzero are the following

$$\underline{M}'_{e1\lambda}(h_1, \underline{r}'_D) = -\frac{\lambda}{2} e^{ih_1z'} \hat{a}_y \qquad (56)$$

$$\underline{M}'_{o1\lambda}(h_1, \underline{r}'_D) = \frac{\lambda}{2} e^{ih_1z'} \hat{a}_x \qquad (57)$$

$$\underline{N}'_{eo\lambda}(h_1, \underline{r}'_D) = \frac{\lambda^2}{k_o^2} e^{ih_1z'} \hat{a}_z \qquad (58)$$

$$\underline{N}_{e1\lambda}(h_1, \underline{r}'_D) = i \frac{h_1\lambda}{2k_o} e^{ih_1z'} \hat{a}_x \qquad (59)$$

$$\underline{N}'_{o1\lambda}(h_1, \underline{r}'_D) = i \frac{h_1\lambda}{2k_o} e^{ih_1z'} \hat{a}_y \qquad (60)$$

Accordingly equations 33 and 41 reduce to the following finite sums in the D coordinate system

$$\overline{\overline{G}}_{3s}^{(11)}(\underline{r}_D, \underline{r}'_D) = \frac{i}{4\pi} \int_0^\infty \frac{d\lambda}{\lambda h_1} 2\left\{ a\left(\underline{M}_{e1\lambda}(h_1, \underline{r}_D) \underline{M}'_{e1\lambda}(h_1, \underline{r}'_D) \right.\right.$$

$$\left. + \underline{M}_{o1\lambda}(h_1, \underline{r}_D) \underline{M}'_{o1\lambda}(h_1, \underline{r}'_D) \right)$$

$$+ b\left(\frac{1}{2} N_{eo\lambda}(h_1, \underline{r}_D) N'_{eo\lambda}(h_1, \underline{r}'_D) \right.$$

$$+ N_{e1\lambda}(h_1, \underline{r}_D) N'_{e1\lambda}(h_1, \underline{r}'_D)$$

$$\left.\left. + N_{o1\lambda}(h_1, \underline{r}_D) \underline{N}'_{o1\lambda}(h_1, \underline{r}'_D) \right)\right\} \qquad (61)$$

24

and

$$\bar{\bar{K}}_s(\underline{r}_D, \underline{r}'_D) = \frac{ik_o}{4\pi} \int\limits_0^\infty \frac{d\lambda}{\lambda h_1} \left\{ a\left(\underline{N}_{e1\lambda}(h_1, \underline{r}_D) \ \underline{M}'_{e1\lambda}(h_1, \underline{r}'_D)\right.\right.$$

$$+ \ \underline{N}_{o1\lambda}(h_1, \underline{r}_D) \ \underline{M}'_{o1\lambda}(h_1, \underline{r}'_D)\Big)$$

$$+ \ b\left(\frac{1}{2} \ \underline{M}_{eo\lambda}(h_1, \underline{r}_D) \ \underline{N}'_{eo\lambda}(h_1, \underline{r}'_D)\right.$$

$$+ \ M_{e1\lambda}(h_1, \underline{r}_D) \ \underline{N}'_{e1\lambda}(h_1, \underline{r}'_D)$$

$$\left.\left.+ \ M_{o1\lambda}(h_1, \underline{r}_D) \ N'_{o1\lambda}(h_1, \underline{r}'_D)\right)\right\} \tag{62}$$

The remaining expressions necessary to make equations 61 and 62 explicit are given by

$$\underline{M}_{eo\lambda}(h_1, \underline{r}_D) = \lambda J_1(\lambda \rho_D) \ e^{ih_1 z} \ \hat{a}_{\phi_D} \tag{63}$$

$$\underline{M}_{e1\lambda}(h_1, \underline{r}_D) = - \ \frac{J_1(\lambda \rho_D)}{\rho_D} \sin \phi_D \ e^{ih_1 z} \ \hat{a}_{\rho_D}$$

$$+ \left(\frac{J_1(\lambda \rho_D)}{\rho_D} - \lambda J_o(\lambda \rho_D)\right) \cos \phi_o \ e^{ih_1 z} \ \hat{a}_{\phi_D}$$

$$\tag{64}$$

25

$$\underline{M}_{o1\lambda}(h_1, \underline{r}_D) = \frac{J_1(\lambda\rho_D)}{\rho_D} \cos \phi_D \, e^{ih_1 z} \, \hat{a}_{\rho_D}$$

$$+ \left(\frac{J_1(\lambda\rho_D)}{\rho_D} - \lambda J_o(\lambda\rho_D) \right) \sin \phi_D \, e^{ih_1 z} \, \hat{a}_{\phi_D} \qquad (65)$$

$$\underline{N}_{eo\lambda}(h_1, \underline{r}_D) = \frac{\lambda^2}{k_o} J_o(\lambda\rho_D) \, e^{ih_1 z} \, \hat{a}_z - i \frac{h_1 \lambda}{k_o} J_1(\lambda\rho_D) \, e^{ih_1 z} \, \hat{a}_{\rho_D} \qquad (66)$$

$$\underline{N}_{e1\lambda}(h_1, \underline{r}_D) = \frac{\lambda^2}{k_o} J_1(\lambda\rho_D) \cos \phi_D \, e^{ih_1 z} \, \hat{a}_z$$

$$+ \frac{ih_1}{k_o} \left(\lambda J_o(\lambda\rho_D) - \frac{J_1(\lambda\rho_D)}{\rho_D} \right) \cos \phi_D \, e^{ih_1 z} \, \hat{a}_{\rho_D}$$

$$- \frac{ih_1}{k_o} \frac{J_1(\lambda\rho_D)}{\rho_D} \sin \phi_D \, e^{ih_1 z} \, \hat{a}_{\phi_D} \qquad (67)$$

$$\underline{N}_{o1\lambda}(h_1, \underline{r}_D) = \frac{\lambda^2}{k_o} J_1(\lambda\rho_D) \sin \phi_D \, e^{ih_1 z} \, \hat{a}_z$$

$$+ \frac{ih_1}{k_o} \left(\lambda J_o(\lambda\rho_D) - \frac{J_1(\lambda\rho_D)}{\rho_D} \right) \sin \phi_D \, e^{ih_1 z} \, \hat{a}_{\rho_D}$$

$$+ \frac{ih_1}{k_o} \frac{J_1(\lambda\rho_D)}{\rho_D} \cos \phi_D \, e^{ih_1 z} \, \hat{a}_{\phi_D} \qquad (68)$$

To obtain $\overline{\overline{G}}_{3s}(\underline{r}, \underline{r}')$ and $\overline{\overline{K}}_s(\underline{r}, \underline{r}')$ we use prescriptions 51 and 52 in conjunction with transformation equations 53 through 55 and

$$\left. \begin{array}{l} \rho_D = |\underline{\rho} - \underline{\rho}'| \\[6pt] \hat{a}_{\rho_D} = \dfrac{\underline{\rho} - \underline{\rho}'}{\rho_D} \\[6pt] \hat{a}_{\phi_D} = \hat{a}_z \times \hat{a}_{\rho_D} \end{array} \right\} \qquad (69)$$

26

We are now in a position to rewrite the EFIDE and MFIE operators as the sum of three terms as we stated in the abstract. The first term describes free-field interaction, the sum of the first two describes interaction above a perfectly conducting ground and, naturally, the sum of all three terms describes interaction above a finitely conducting ground. The corresponding decomposition for the source term will be given in the next section.

Equations 31 and 37 represent the first stage of the decomposition, i.e., the free-field interaction term has been separated from the scattering form. Thus we must further decompose the scattering term. Recalling equations 61, 62 and subsequent equations 63 through 68 we can cast $\overline{\overline{G}}_{3s}(\underline{r}_D, \underline{r}'_D)$ and $\overline{\overline{K}}_s(\underline{r}_D, \underline{r}'_D)$ into the following forms

$$\overline{\overline{G}}_{3s}(\underline{r}_D, \underline{r}'_D) = G_{3s\rho\rho}\, \hat{a}_{\rho_D}\, \hat{a}_{\rho_D} + G_{3s\phi\phi}\, \hat{a}_{\phi_D}\, \hat{a}_{\phi_D} + G_{3s\rho z}\, \hat{a}_{\rho_D}\, \hat{a}_z$$

$$+ G_{3sz\rho}\, \hat{a}_z\, \hat{a}_{\rho_D} + G_{3szz}\, \hat{a}_z\, \hat{a}_z \tag{70}$$

$$\overline{\overline{K}}_s(\underline{r}_D, \underline{r}'_D) = K_{s\rho\phi}\, \hat{a}_{\rho_D}\, \hat{a}_{\phi_D} + K_{s\phi\rho}\, \hat{a}_{\phi_D}\, \hat{a}_{\rho_D} + K_{sz\phi}\, \hat{a}_z\, \hat{a}_{\phi_D}$$

$$+ K_{s\phi z}\, \hat{a}_{\phi_D}\, \hat{a}_z \tag{71}$$

where

$$G_{3s\rho\rho} = \frac{1}{4\pi k_o^2}\left[\frac{\partial^2}{\partial\rho_D^2}(-G_{21} + k_o^2 V_{22}) + k_o^2(-G_{21} + U_{22})\right] \tag{72a}$$

$$G_{3s\phi\phi} = \frac{1}{4\pi k_o^2}\left[\frac{1}{\rho_D}\frac{\partial}{\partial\rho_D}(-G_{21} + k_o^2 V_{22}) + k_o^2(-G_{21} + U_{22})\right] \tag{72b}$$

$$G_{3s\rho z} = \frac{1}{4\pi k_o^2}\left[\frac{\partial^2}{\partial\rho_D\,\partial z}(-G_{21} + k^2 V_{22})\right] = -G_{3sz\rho} \tag{72c}$$

27

$$G_{3szz} = \frac{1}{4\pi k_o^2} \left[\left(\frac{\partial^2}{\partial z^2} + k_o^2 \right) (-G_{21} + k^2 V_{22}) \right] \tag{72d}$$

$$K_{s\rho\phi} = \frac{1}{4\pi} \left[\frac{\partial}{\partial z} (G_{21} - U_{22}) + \frac{1}{\rho_D} \frac{\partial}{\partial \rho_D} W_{22} \right] \tag{72e}$$

$$K_{s\phi\rho} = \frac{1}{4\pi} \left[\frac{\partial}{\partial z} (-G_{21} + U_{22}) - \frac{\partial^2}{\partial \rho_D^2} W_{22} \right] \tag{72f}$$

$$K_{sz\phi} = \frac{1}{4\pi} \left[\frac{\partial}{\partial \rho_D} (-G_{21} + U_{22}) \right] \tag{72g}$$

$$K_{s\phi z} = \frac{1}{4\pi} \left[\frac{\partial}{\partial \rho_D} (G_{21} - k^2 V_{22}) \right] \tag{72h}$$

where

$$G_{21} = \frac{e^{ik_o R_+}}{R_+} = \int_0^\infty \frac{ie^{ih_1(z+z')}}{h_1} J_o(\lambda \rho_D) \lambda \, d\lambda$$

$$R_+ = \left[(z + z')^2 + \rho_D^2 \right]^{1/2} \tag{73a}$$

$$V_{22} = \int_0^\infty \frac{2ie^{ih_1(z+z')}}{k^2 h_1 + k_o^2 h_2} J_o(\lambda \rho_D) \lambda \, d\lambda \tag{73b}$$

$$U_{22} = \int_0^\infty \frac{2ie^{ih_1(z+z')}}{h_1 + h_2} J_o(\lambda \rho_D) \lambda \, d\lambda \tag{73c}$$

$$W_{22} = \int_0^\infty \frac{2(h_1 - h_2) e^{ih_1(z+z')}}{k^2 h_1 + k_o^2 h_2} J_o(\lambda \rho_D) \lambda \, d\lambda \tag{73d}$$

The above integrals are well studied and can be found in reference 3 where the same symbols are used with a slightly different but equivalent representation for the integrands.

28

To proceed with the decomposition we consider the limit as conductivity σ of the ground becomes infinite. One can show that

$$\lim_{k \to \infty} k^2 V_{22} = 2G_{21}, \quad \lim_{k \to \infty} U_{22} = 0, \quad \lim_{k \to \infty} V_{22} = 0, \quad \lim_{k \to \infty} W_{22} = 0$$

and equations 72 in this limit becomes

$$G^P_{3s\rho\rho} = -\frac{1}{4\pi k^2_o}\left[\left(\frac{\partial^2}{\partial \rho^2_D} + k^2_o\right) G_{21}\right] \tag{74a}$$

$$G^P_{3s\phi\phi} = -\frac{1}{4\pi k^2_o}\left[\left(\frac{1}{\rho_D}\frac{\partial}{\partial \rho_D} + k^2_o\right) G_{21}\right] \tag{74b}$$

$$G^P_{3s\rho z} = \frac{1}{4\pi k^2_o}\left[\frac{\partial^2}{\partial \rho_D \partial z} G_{21}\right] = -G^P_{3sz\rho} \tag{74c}$$

$$G^P_{3szz} = \frac{1}{4\pi k^2_o}\left[\left(\frac{\partial^2}{\partial z^2} + k^2_o\right) G_{21}\right] \tag{74d}$$

$$K^P_{s\rho\phi} = \frac{1}{4\pi}\frac{\partial G_{21}}{\partial z} = -K^P_{s\phi\rho} \tag{74e}$$

$$K^P_{sz\phi} = -\frac{1}{4\pi}\frac{\partial G_{21}}{\partial \rho_D} = K^P_{s\phi z} \tag{74f}$$

where the superscript P means perfectly conducting. By regrouping terms in equations 72 and utilizing equations 74, we obtained the following decomposition

$$\bar{\bar{G}}_{3s} = \bar{\bar{G}}^P_{3s} + \bar{\bar{G}}^F_{3s} \tag{75}$$

$$\bar{\bar{K}}_s = \bar{\bar{K}}^P_s + \bar{\bar{K}}^F_s \tag{76}$$

29

where the elements of $\overline{\overline{G}}_{3s}^P$ and $\overline{\overline{K}}_s^P$ are given by equations 74 and the elements of $\overline{\overline{G}}_{3s}^F$ and $\overline{\overline{K}}_s^F$ (F stands for finitely conducting) are given by

$$G_{3s\rho\rho}^F = \frac{1}{4\pi}\left[\frac{\partial^2 V_{22}}{\partial \rho_D^2} + U_{22}\right] \tag{77a}$$

$$G_{3s\phi\phi}^F = \frac{1}{4\pi}\left[\frac{1}{\rho_D}\frac{\partial V_{22}}{\partial \rho_D} + U_{22}\right] \tag{77b}$$

$$G_{3s\rho z}^F = \frac{1}{4\pi k_o^2}\left[\frac{\partial^2}{\partial \rho_D \partial z}(k^2 V_{22} - 2G_{21})\right] = -G_{3sz\rho}^F \tag{77c}$$

$$G_{3szz}^F = \frac{1}{4\pi k_o^2}\left[\left(\frac{\partial^2}{\partial z^2} + k_o^2\right)(k^2 V_{22} - 2G_{21})\right] \tag{77d}$$

$$K_{s\rho\phi}^F = \frac{1}{4\pi}\left[-\frac{\partial U_{22}}{\partial z} + \frac{1}{\rho_D}\frac{\partial}{\partial \rho_D}W_{22}\right] \tag{77e}$$

$$K_{s\phi\rho}^F = \frac{1}{4\pi}\left[\frac{\partial U_{22}}{\partial z} - \frac{\partial^2}{\partial \rho_D^2}W_{22}\right] \tag{77f}$$

$$K_{sz\phi}^F = \frac{1}{4\pi}\frac{\partial U_{22}}{\partial \rho_D} \tag{77g}$$

$$K_{s\phi z}^F = \frac{1}{4\pi}\left[\frac{\partial}{\partial \rho_D}(2G_{21} - k^2 V_{22})\right]. \tag{77h}$$

Thus by invoking equations 31, 37, 75 and 76 we can complete the promised decomposition:

$$\overline{\overline{G}}_{3s} = \overline{\overline{G}}_o + \overline{\overline{G}}_{3s}^P + \overline{\overline{G}}_{3s}^F \tag{78}$$

$$\overline{\overline{K}}_s = \overline{\overline{K}}_o + \overline{\overline{K}}_s^P + \overline{\overline{K}}_s^F \tag{79}$$

30

where $\bar{\bar{G}}_o$, $\bar{\bar{K}}_o$ are given by equations 32 and 38 respectively, the elements of $\bar{\bar{G}}^P_{3s}$ and $\bar{\bar{K}}^P_s$ by equations 74 and the elements of $\bar{\bar{G}}^F_{3s}$ and $\bar{\bar{K}}^F_s$ by equations 77.

As a check to the above calculations we should arrive at equations 74 by employing the standard forms for $\bar{\bar{G}}^P$ and $\bar{\bar{K}}^P$. These represent the scattered parts for interaction above a perfectly conducting ground and are given by the well known expressions

$$\bar{\bar{G}}^P_s = \left(\underline{\underline{I}} + \frac{1}{k_o^2} \nabla\nabla \right) \cdot \left(-g_o(z' \to -z') \underline{\underline{I}} + 2\hat{a}_z \hat{a}_z g_o (z' \to -z') \right) \tag{80}$$

$$\bar{\bar{K}}^P_s = - \frac{1}{4\pi} \nabla G_{21} \times \bar{\bar{I}}_r \tag{81}$$

where g_o is the free space scalar Green's function given by equation 33, G_{21} is defined by equation 73a and $\bar{\bar{I}}_r$ is a reflection operator given by

$$\bar{\bar{I}}_r = \hat{a}_{\rho_D} \hat{a}_{\rho_D} + \hat{a}_{\phi_D} \hat{a}_{\phi_D} - \hat{a}_z \hat{a}_z .$$

It can be shown by some rather lengthy algebraic manipulations that equation 80 is identical to equations 74a through 74d and equation 81 is identical to equations 74e and 74f.

SECTION V

REPRESENTATIONS FOR $\underline{E}_T(\underline{r})$ AND $\underline{H}_T(\underline{r})$

Using equation 16 in conjunction with the coordinate notation changes described to obtain equation 27 and equation 29, we obtain

$$\underline{E}_T(\underline{r}) = i\omega\mu_0 \int_{V_J} \overline{\overline{G}}_3^{(11)}(\underline{r},\underline{r}') \cdot \underline{J}(\underline{r}') \, dV' \qquad (82)$$

and using equations 35, 36, and 82 we obtain

$$\underline{H}_T(\underline{r}) = \int_{V_J} \overline{\overline{K}}(\underline{r},\underline{r}') \cdot \underline{J}(\underline{r}') \, dV'. \qquad (83)$$

As discussed in the previous section, $\underline{E}_T(\underline{r})$ and $\underline{H}_T(\underline{r})$ have meaning in their own right, independent of their role in the appropriate EFIDE or MFIE. They are the total electric and magnetic fields at any point $\underline{r}$ in the lossless medium due to a specified source distribution $\underline{J}(\underline{r}')$, $\underline{r}' \in V_J$, and equations 82 and 83 include all interaction with the lossy half space. The work presented in the previous section enhances the utility of equations 82 and 83 in that the form to be used for $G_3^{(11)}(\underline{r},\underline{r}')$ is the simplified form given by equation 78, while the form to be used for $\overline{\overline{K}}(\underline{r},\underline{r}')$ is the simplified form given by equation 79.

If we now focus our attention on the role of $\underline{E}_T(\underline{r})$ and $\underline{H}_T(\underline{r})$ in the EFIDE and MFIE then we consider two cases. The first case is when we desire to calculate the surface current density induced on the scattering body and the source of excitation is a specified distribution of current that exists somewhere in the lossless medium. For this case we must employ equations 82 and 83 explicitly in conjunction with the EFIDE and MFIE. The second

32

case is one of considerable interest. This is the case when the
source of excitation is an incident plane wave. For this case
we make use of the fact that $\underline{E}_T(\underline{r})$ and $\underline{H}_T(\underline{r})$ are simply the
incident plus reflected fields from the lossy half-space and
we do not have to explicitly evaluate equations 82 and 83.
For completeness we will present explicit representations for
this case. These representations are obtained in the standard
manner in which the incident field is decomposed so that it
is the superposition of two component fields. One component
field has its electric field polarized perpendicular to the
plane of incident, and the other component field has its
magnetic field polarized perpendicular to the plane of inci-
dence. The analysis leading to the results is straightforward
after the described decomposition is employed. For an inci-
dent field given by

$$\underline{E}_i = \hat{e}\, E_o\, e^{ik_o \hat{n}_o \cdot \underline{r}} \tag{84}$$

with $\hat{e}$ being a unit vector along the polarization direction and
$\hat{n}_o$ being a unit vector in the propagation direction, the total
fields are

$$\underline{E}_T = \underline{E}_i + \underline{E}^P + \underline{E}^F \tag{85}$$

and

$$\underline{H}_T = \underline{H}_i + \underline{H}^P + \underline{H}^F \tag{86}$$

where

$$\underline{H}_i = (E_o/Z_o)(\hat{n}_o \times \hat{e})\, e^{ik_o \hat{n}_o \cdot \underline{r}} \tag{87}$$

$$\underline{E}^P = -E_o \left[(\hat{e} \cdot \hat{h})\hat{h} + (\hat{e} \cdot \hat{v})(\hat{n}_R \times \hat{h}) \right] e^{ik_o \hat{n}_R \cdot \underline{r}} \tag{88a}$$

33

$$\underline{E}^F = E_o\left[(R_H + 1)(\hat{e} \cdot \hat{h})\hat{h} - (R_V - 1)(\hat{e} \cdot \hat{v})(\hat{n}_R \times \hat{h})\right]$$

$$e^{ik_o\hat{n}_R\cdot\underline{r}} \qquad (88b)$$

$$\underline{H}^P = -(E_o/Z_o)\left[(\hat{e} \cdot \hat{h})(\hat{n}_R \times \hat{h}) - (\hat{e} \cdot \hat{v})\hat{h}\right]e^{ik_o\hat{n}_R\cdot\underline{r}} \qquad (88c)$$

$$\underline{H}^F = (E_o/Z_o)\left[(R_H + 1)(\hat{e} \cdot \hat{h})(\hat{n}_R \times \hat{h}) + (R_V - 1)(\hat{e} \cdot \hat{v})\hat{h}\right]$$

$$e^{ik_o\hat{n}_R\cdot\underline{r}} \qquad (88d)$$

$$\hat{h} = \frac{\hat{n}_o \times \hat{a}_z}{|\hat{n}_o \times \hat{a}_z|} \qquad (\text{If } \hat{n}_o = -\hat{a}_z \text{ then } \hat{h} = \hat{a}_y)$$

$$\hat{v} = \hat{h} \times \hat{n}_o \qquad (89)$$

$$\hat{n}_R = \hat{n}_o \cdot (\underline{\underline{I}} - 2\hat{a}_z\hat{a}_z)$$

$$R_H = \frac{-k_o(\hat{a}_z \cdot \hat{n}_o) - \left[k^2 - k_o^2(1 - (\hat{a}_z \cdot \hat{n}_o)^2)\right]^{1/2}}{-k_o(\hat{a}_z \cdot \hat{n}_o) + \left[k^2 - k_o^2(1 - (\hat{a}_z \cdot \hat{n}_o)^2)\right]^{1/2}}$$

$$\qquad (90)$$
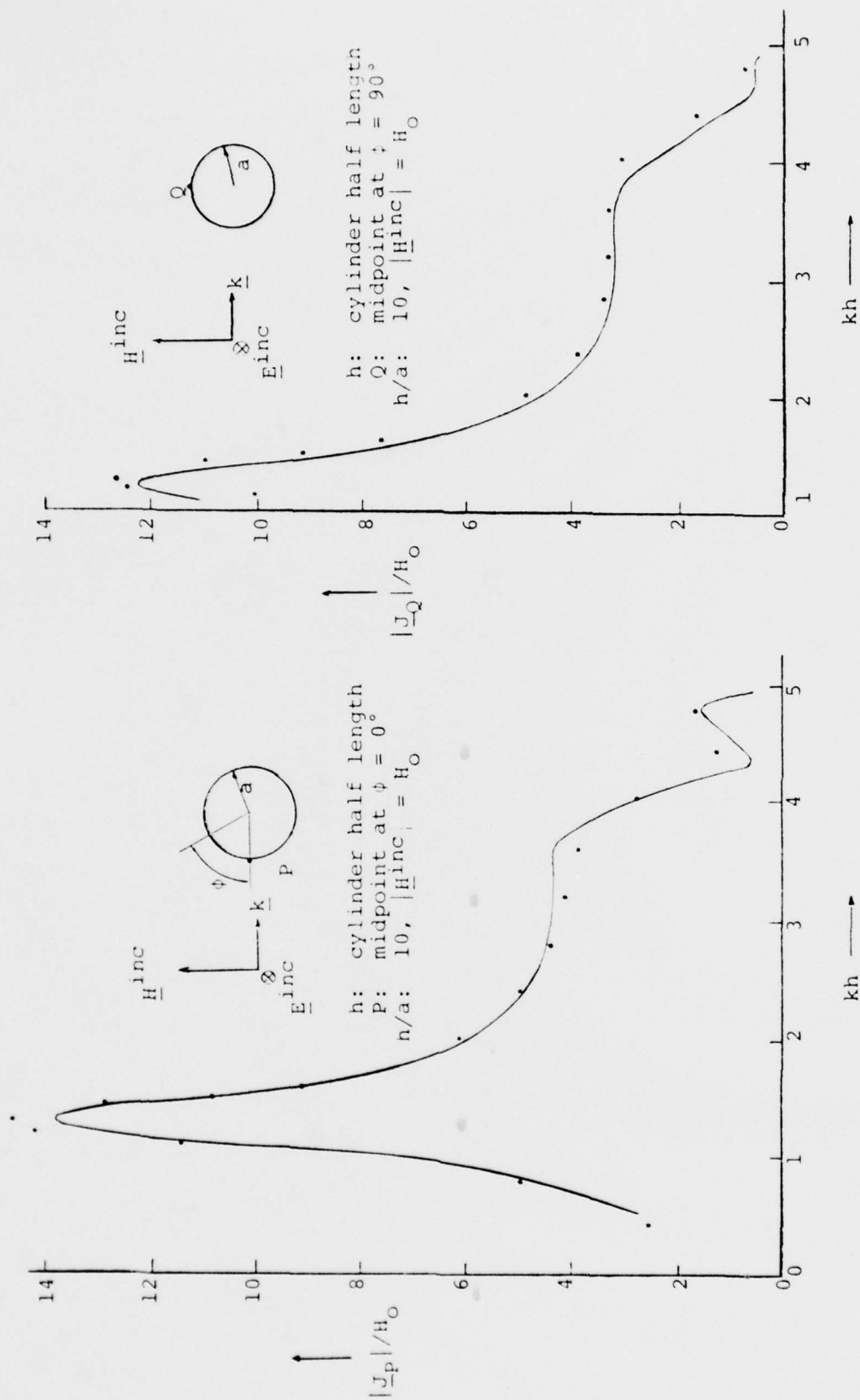
$$R_V = \frac{-k^2(\hat{a}_z \cdot \hat{n}_o) - k_o\left[k^2 - k_o^2(1 - (\hat{a}_z \cdot \hat{n}_o)^2)\right]^{1/2}}{-k^2(\hat{a}_z \cdot \hat{n}_o) + k_o\left[k^2 - k_o^2(1 - (\hat{a}_z \cdot \hat{n}_o)^2)\right]^{1/2}}$$

R_H and R_V are the usual Fresnel reflection coefficients
so the square root is defined to have a positive real part.
We note that as the conductivity of the half-space approaches
infinity, then $R_H \to -1$ and $R_V \to 1$. It can now be seen that
in this limit $\underline{E}^F$ and $\underline{H}^F$ vanish and this was the reason for the
decomposition of $\underline{E}_T$ and $\underline{H}_T$ as expressed in equations 85 and 86.

34

The first two terms in these expressions represent the total fields, incident plane reflected due to the presence of a perfectly conducting half-space. The addition of $\underline{E}^F$ and $\underline{H}^F$ to the "perfectly conducting" total fields, yields an exact representation for the total fields, $\underline{E}^T$ and $\underline{H}^T$, resulting from the presence of the finitely conducting half-space.

SECTION IV
COMPARISON BETWEEN NUMERICAL AND EXPERIMENTAL
DATA FOR METALLIC OBJECTS IN FREE SPACE AND
ABOVE A PERFECTLY CONDUCTING GROUND

In this section we compare numerical data derived via our Magnetic Field Integral Equation (MFIE) Code to experimental data obtained at the University of Michigan. The quantity of interest is the magnitude of the current density induced on metallic objects in free space and in the presence of a perfectly conducting ground by a monochromatic plane wave. In particular we considered a perfectly conducting circular cylinder in free space and also above a perfectly conducting ground and a perfectly conducting aircraft model in free space. Thus figure 3 presents the comparison for the magnitude of the induced current density as a function of kh (k being the free space wave number and h the halflength of the cylinder) at the two points P and Q indicated on the graphs. The incident wave is polarized with its electric vector parallel to the axis and the propagation vector $\underline{k}$ is perpendicular to the axis. The agreement is generally very good. Notice that the peak value obtained via the MFIE code is higher than the one measured at the University of Michigan. This is in agreement with the results obtained by Sassman (ref. 9) who calculated the total current I as a function of kh. Sassman obtained 84a for the peak value of the I/H_o and this should be smaller than $2\pi a |J_P|/H_o$ since $|J_P|$ is maximum at P. The code gives $2\pi a |J_P| \approx 89a$ and the measured data gives 84a. (Figures 4 and 5 are taken from the University of Michigan report since the solid curves in figure 3 are our smoothed out drawings for the original graphs in figures 4 and 5 and as such they are subjective.)
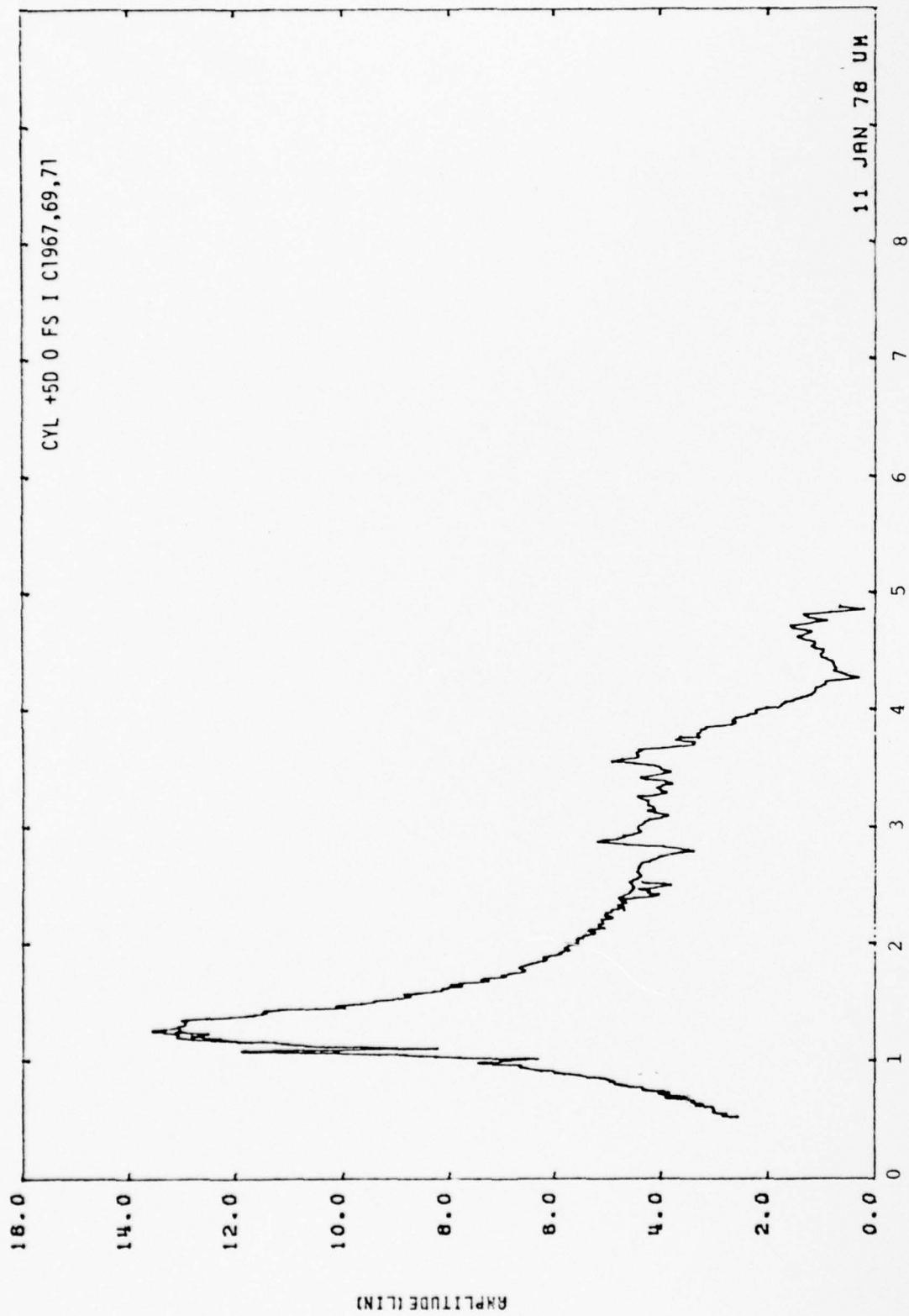
36

Figure 3a,b. Comparison Between "Free Cylinder" Experimental Results at University of Michigan (Solid Curves) and TDR's Code (Dots).

37

CYL +5D 0 FS I C1967,69,71

11 JAN, 78 UM

AMPLITUDE(LIN)

Figure 4. The University of Michigan Original Plot for the Solid Curve in Figure 3a.

38

CYL +5D 80 FS I C1857.55

11 JAN 78 UM

16.0   14.0   12.0   10.0   8.0   6.0   4.0   2.0   0.0

AMPLITUDE (LIN)

0   1   2   3   4   5   6   7   8
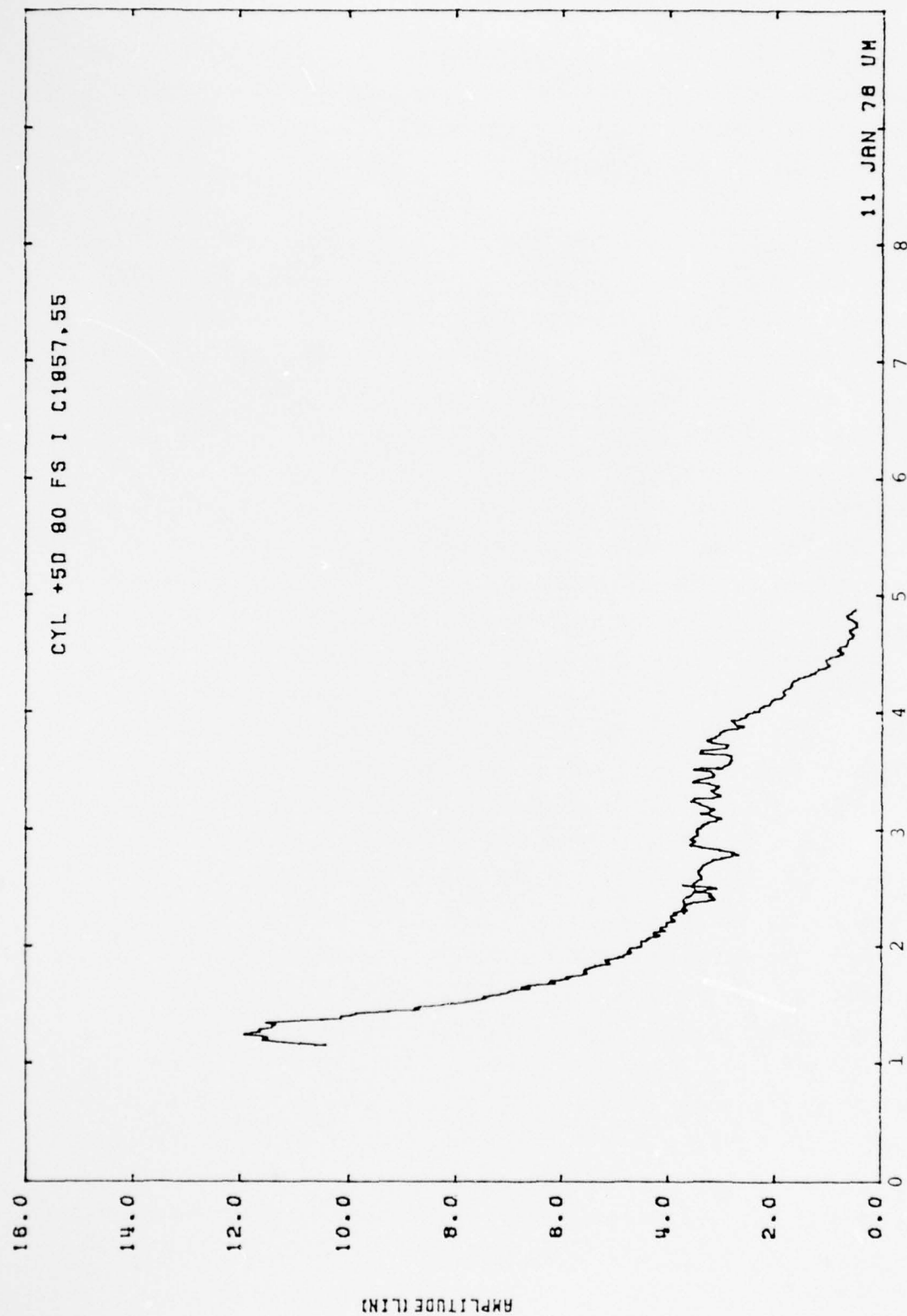
Figure 5. The University of Michigan Original Plot
for the Solid Curve in Figure 3b.

In Figure 6 the cylinder is situated above a perfectly conduct-
ing ground with its axis parallel to the ground. The incident
field is the same as in Figure 3 and the distance of the cylin-
der axis from the plane is 5a.

Again, Figure 7 refers to the original graph in the Univer-
sity of Michigan report. Figure 8 depicts the same situation as
in Figure 6 except that the cylinder axis is much closer to the
ground. (Figure 9 is the corresponding graph in the University
of Michigan report.) Notice that the deviation near the two
maxima is much greater than everywhere else. To satisfy our-
selves that the discrepancy between the experimental values
of current density and the corresponding numerical predictions
were not the fault of the finite number of zones used to parti-
tion the surface of the cylinder, we systematically increased the
number of zones until we obtained what appeared to be a con-
verging sequence. For the cylinder in free space and for the
cylinder 5 radii above the perfectly conducting ground plane
we increased the zoning until for each frequency the response
was insensitive to zoning changes. However, the small change
in the predicted resonant frequency due to a change in zoning,
coupled with the sharp resonance for the case in which the
axis of the cylinder was 1.5 radii above the ground plane,
caused the above convergence criterion to be too stringent to
be practical for frequencies near this resonance; instead, in
this region, we required that both the resonant frequency and
the peak value be insensitive to zoning changes.

The zoning scheme that produced the results found in
Figure 8 was 18 zones along the length and 10 zones around
the circumference, while for Figure 6 it was sufficient to use
10 zones along the length and 6 zones around the circumference.
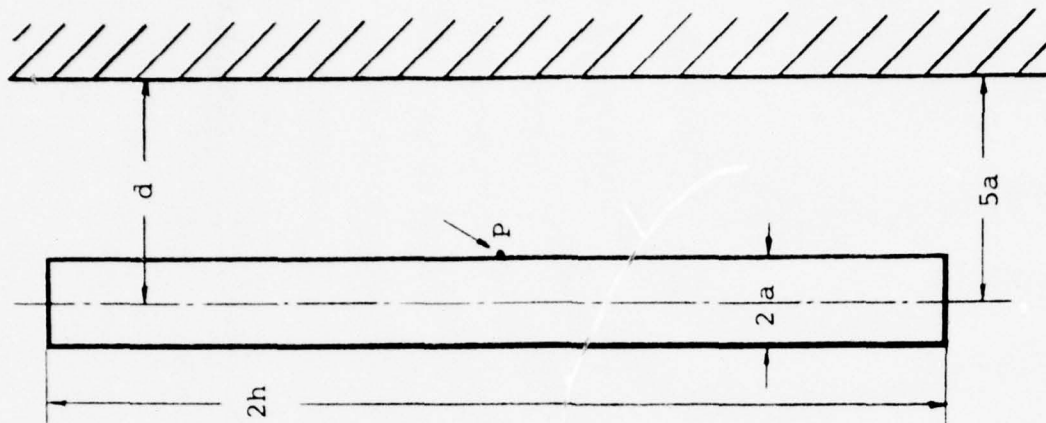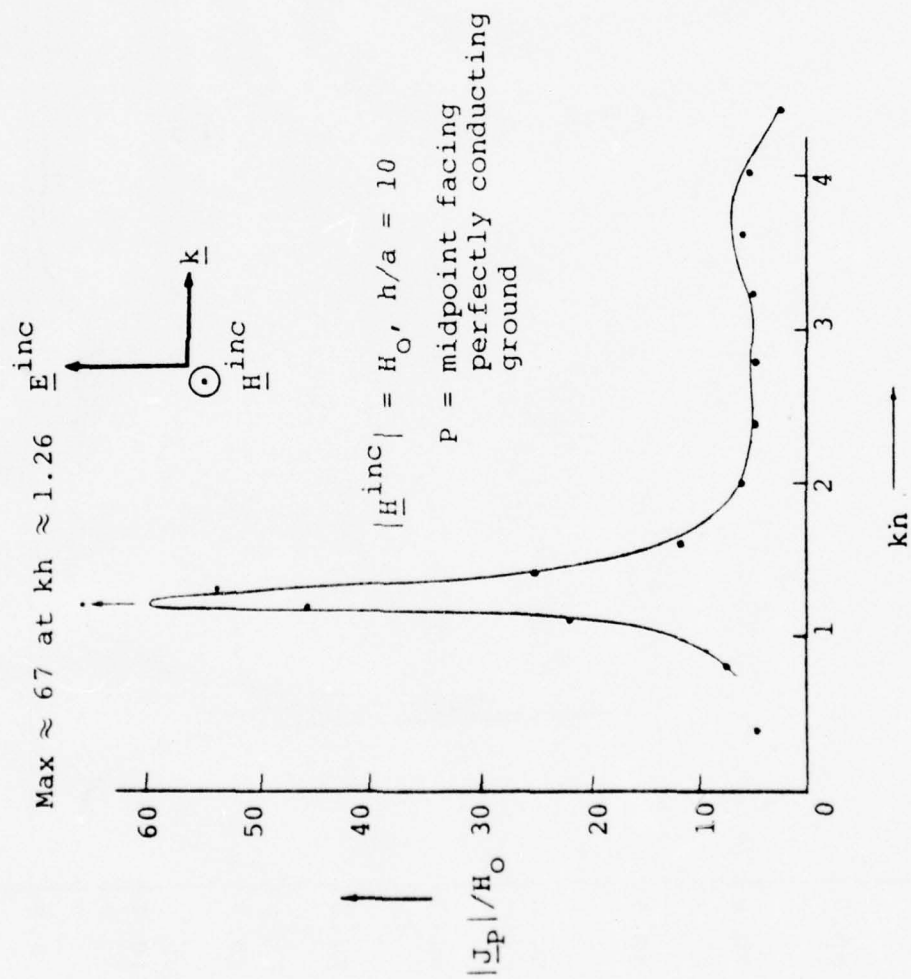In both cases there was one zone along the radius of the endcap.

40

Figure 6. Comparison Between "Cylinder Parallel to a Perfectly Conducting Ground" Experimental Results at University of Michigan (Solid Curve) and TDR's Code (Dots for d = 5a).
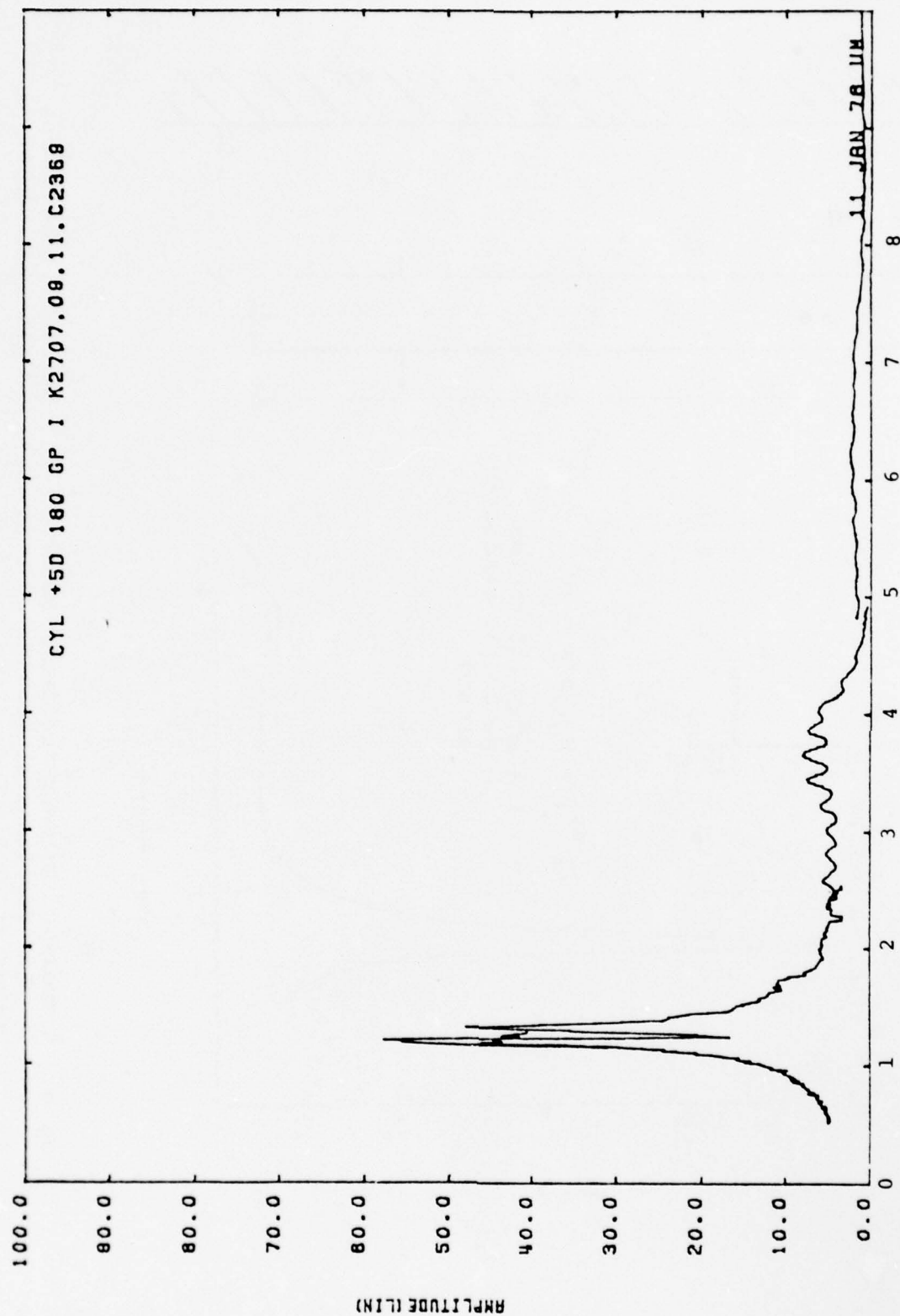
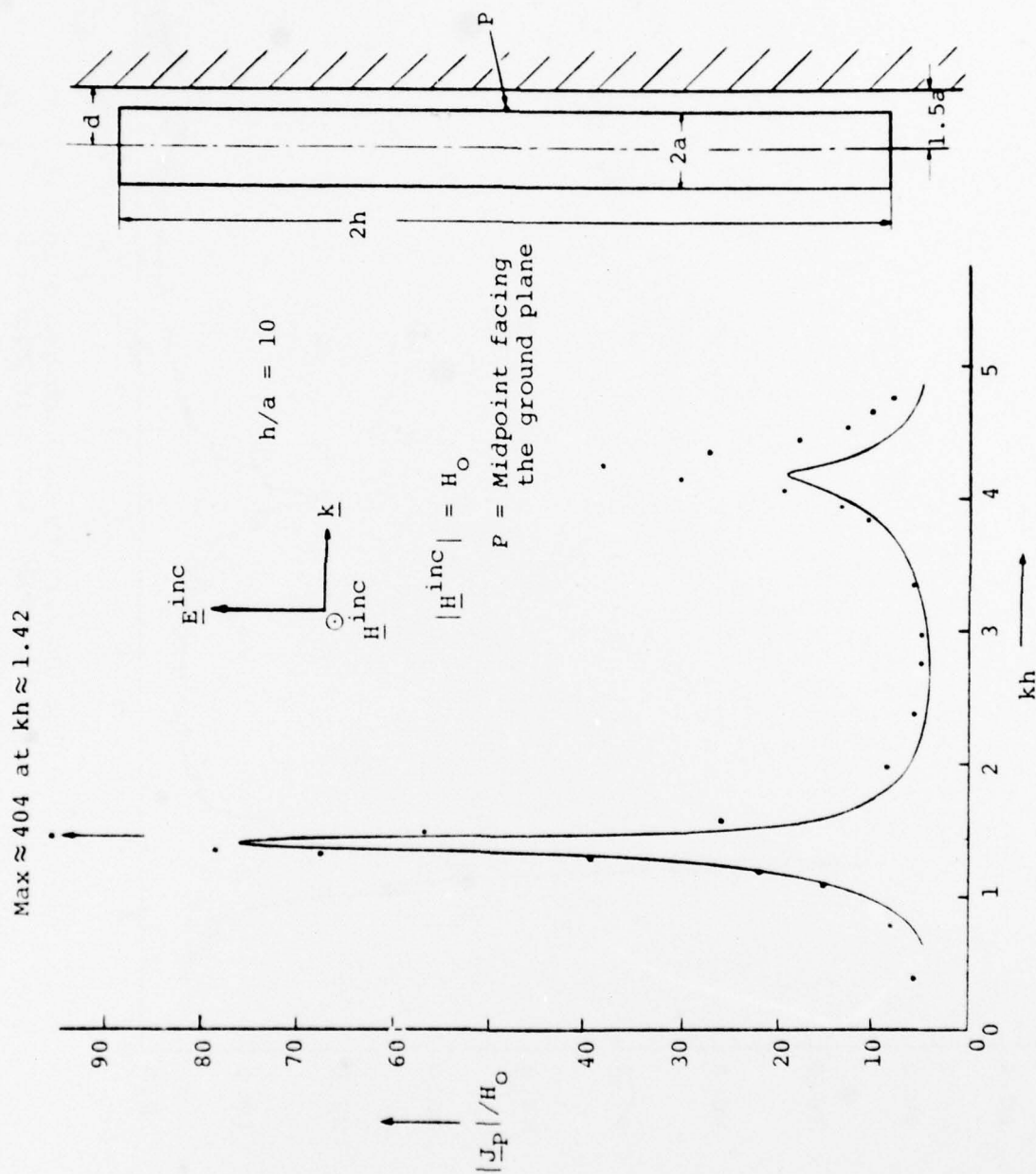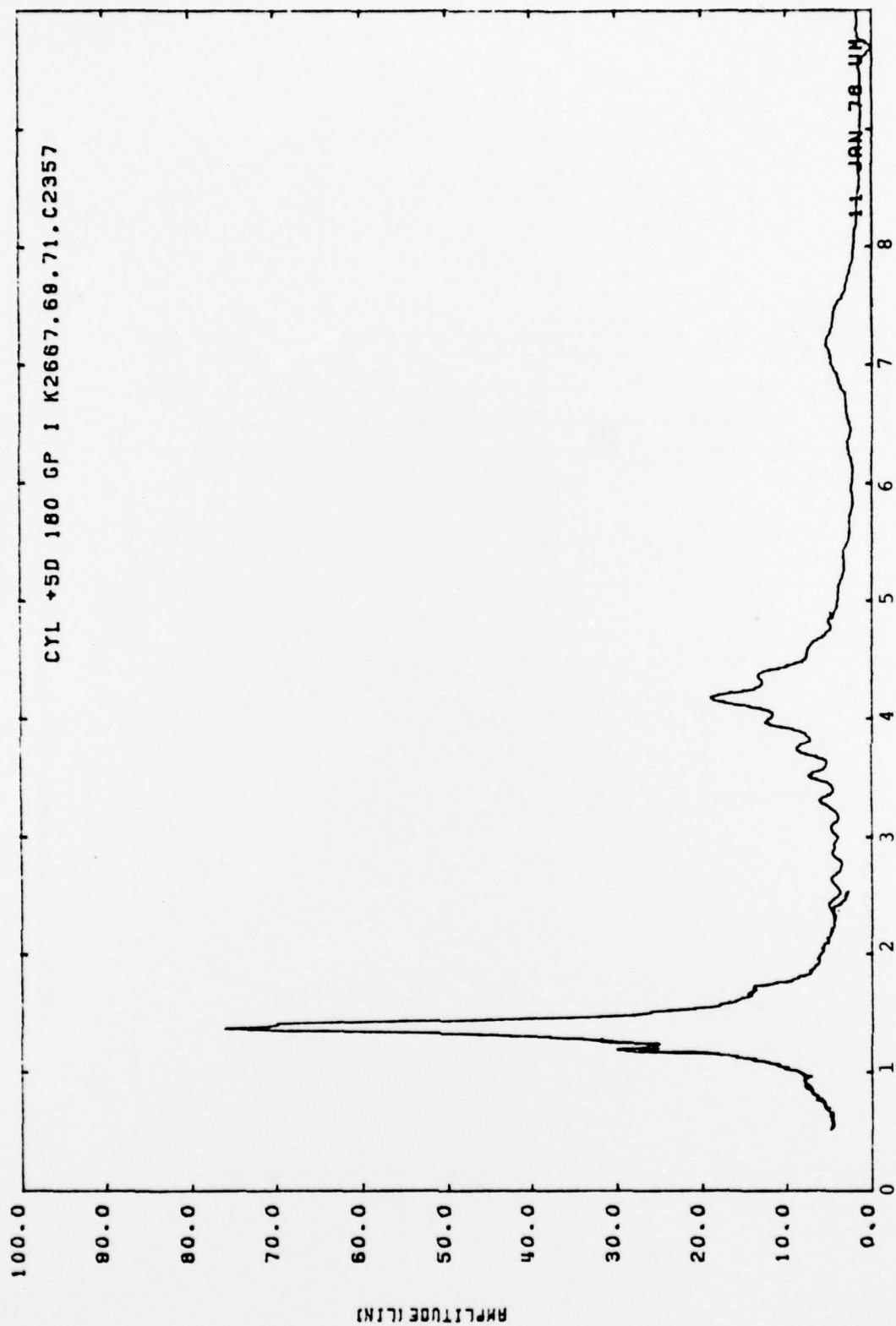Figure 7. The University of Michigan Original Plot for the Solid Curve in Figure 6.

Figure 8. Comparison Between "Cylinder Parallel to Perfectly Conducting Ground" Experimental Results at University of Michigan (Solid Curve) and TDR's Code (Dots) for d = 1.5a.

Figure 9. The University of Michigan Original Plot for the Solid Curve in Figure 8.

Figure 10 is a schematic for the aircraft model considered at the University of Michigan the exact dimensions of which are given in Table 1. The experiments were conducted with the brass scale model; however, our graphs refer to the unscaled aircraft dimensions given in Table 1. Figures 12, 14 and 16 present the comparison for the magnitude of the induced current density along the top of the fuselage for kh = 0.82, 1.694, 20.14, where h is the fuselage halflength. Figures 13, 15, and 17 refer to the bottom of the fuselage. The incident plane wave has its electric vector polarized parallel to the fusalage and the propagation vector perpendicular to the fuselage axis. The distance ℓ(in meters) shown in the graphs is the arclength defined in Figure 11. Notice that the deviation between experimental and theorectical values on the fin (vertical stabilizer) is much greater than on the fuselage. (In figure 13 our results were off scale and are not shown.) A possible explanation for this discrepancy may be based on the fact that the measuring sensors are of finite size and do not pick up the fields right on the surface. This is important because the elliptical cross section of the fin has a ratio $a_v/b_v \approx 6$, i.e., the curvature about the points where the measurements were performed varies rapidly and consequently the fields can change rapidly as we move away from the surface. This is at least true for the special case of a perfectly conducting cylinder of infinite length and elliptical cross section immersed in a magnetostatic field parallel to the minor axis. For this case we found that at a distance (in the direction of the major axis) equal to $0.25\, b_v \approx 0.025$ in (b_v is the minor semi-axis) the azimuthal component of the total magnetic field is equal to half its value on the surface. The above discussion indicates that our higher values on the surface of the fin may actually be compatible with the lower values obtained with the finite size sensors which of necessity measure fields at points off the surface.

Figure 10. Magnetic Field Integral Equation Aircraft Model.

46

Table 1.

MODEL SPECIFICATION

Parameter	Air Force (meters)	U. of Mich. (meters)	U. of Mich. (scaled) (inches)
L	40.00	40.00	6.847
L_f	16.76	16.76	2.869
L_m	17.08	17.08	2.924
L_r	6.16	6.16	1.054
L_w	18.11	18.11	3.100
L_h	4.22	4.22	0.722
L_v	6.5	6.5	1.113
a_f	1.85	1.83	0.313
a_v	3.66	3.651	0.625
b_v	0.73	0.634	0.109
a_h	1.83	1.826	0.313
b_h	0.37	0.317	0.054
a_w	3.00	3.104	0.531
b_w	0.61	0.537	0.092
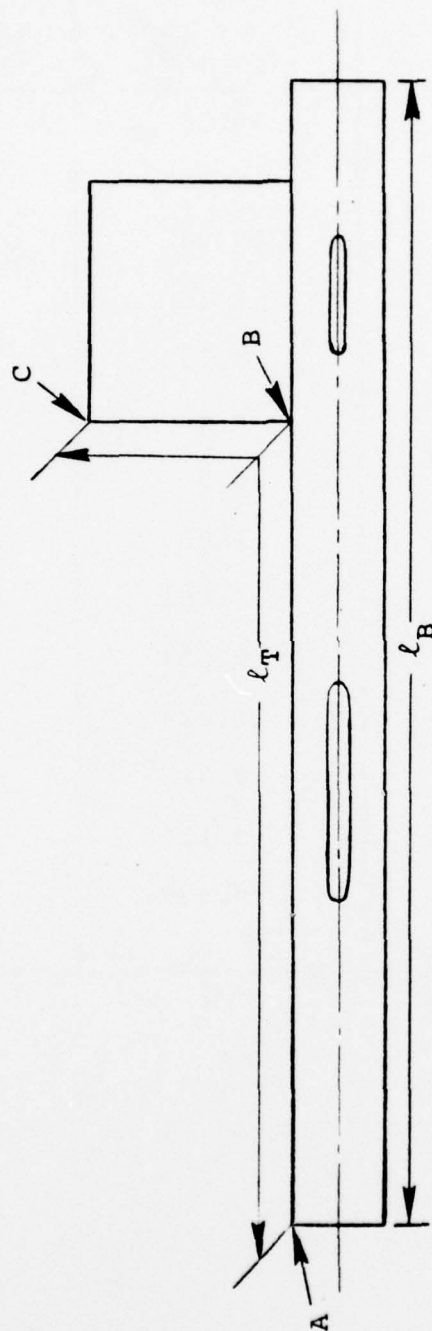
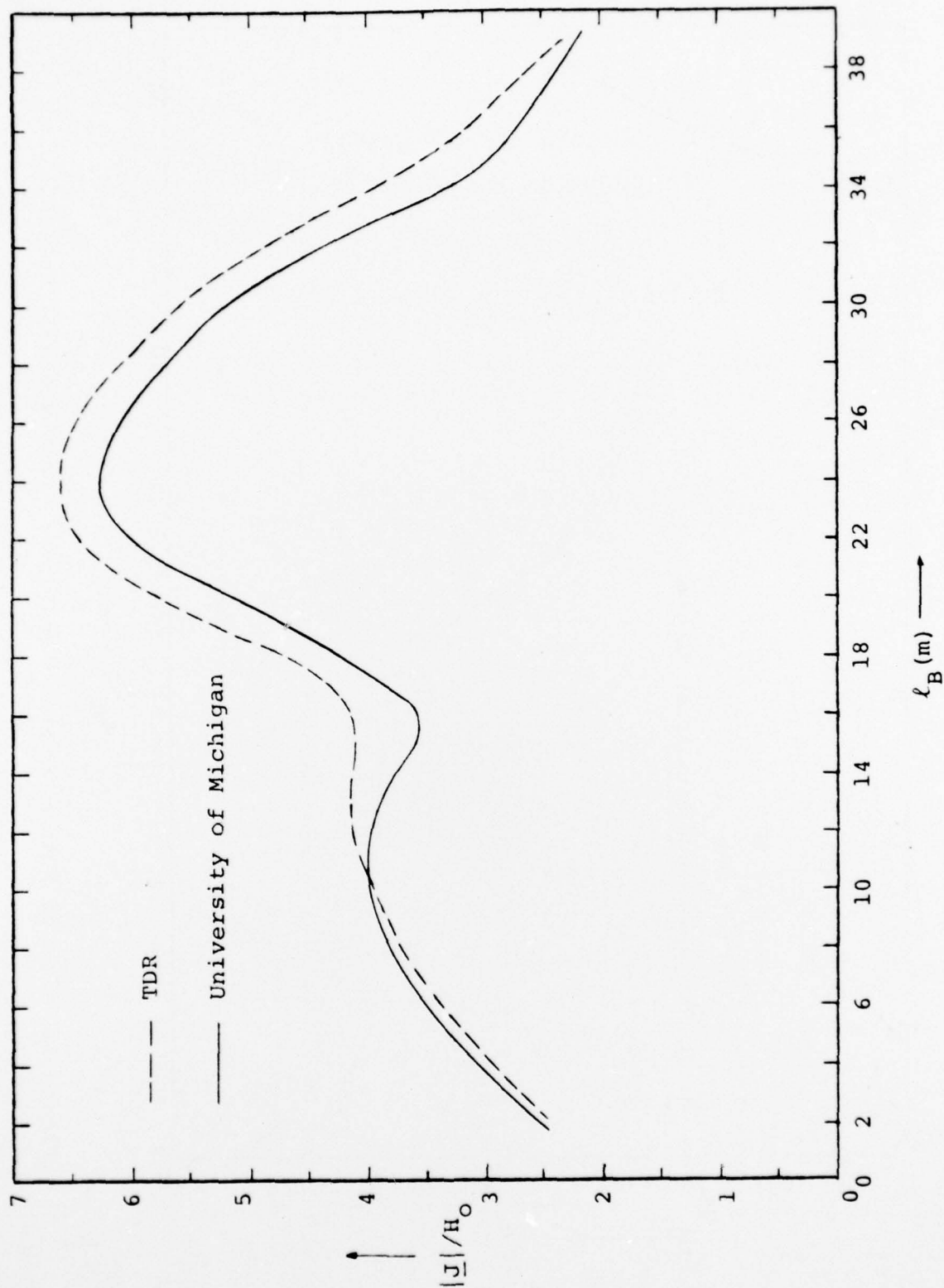Figure 11. Definition of Distances ℓ_T and ℓ_B Used in the Graphs.

48

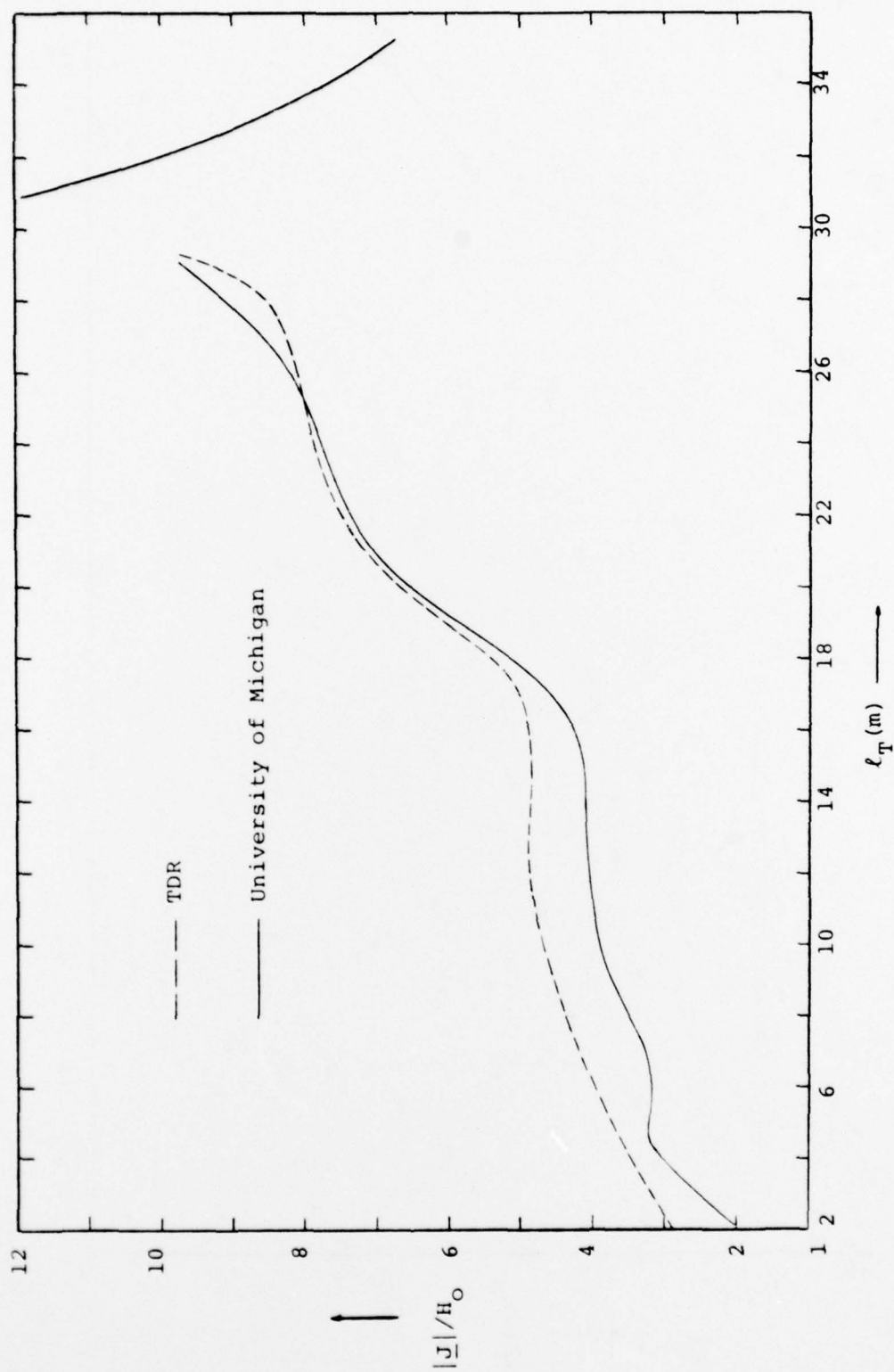Figure 12. Bottom of Fuselage, kh = 0.82. (h: fuselage half length).

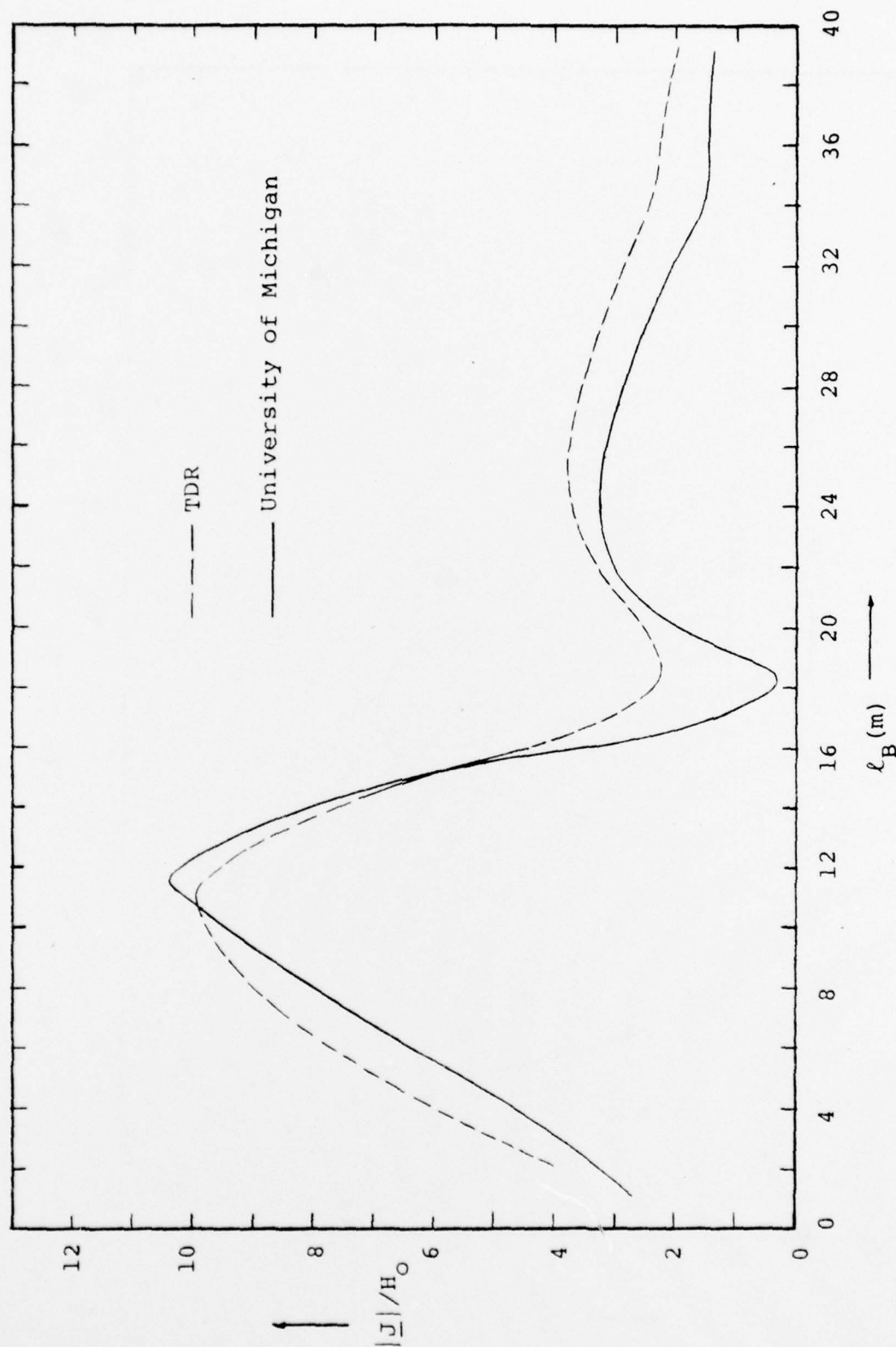Figure 13. Top of Fuselage, kh = 0.82. (h: Fuselage half length.)

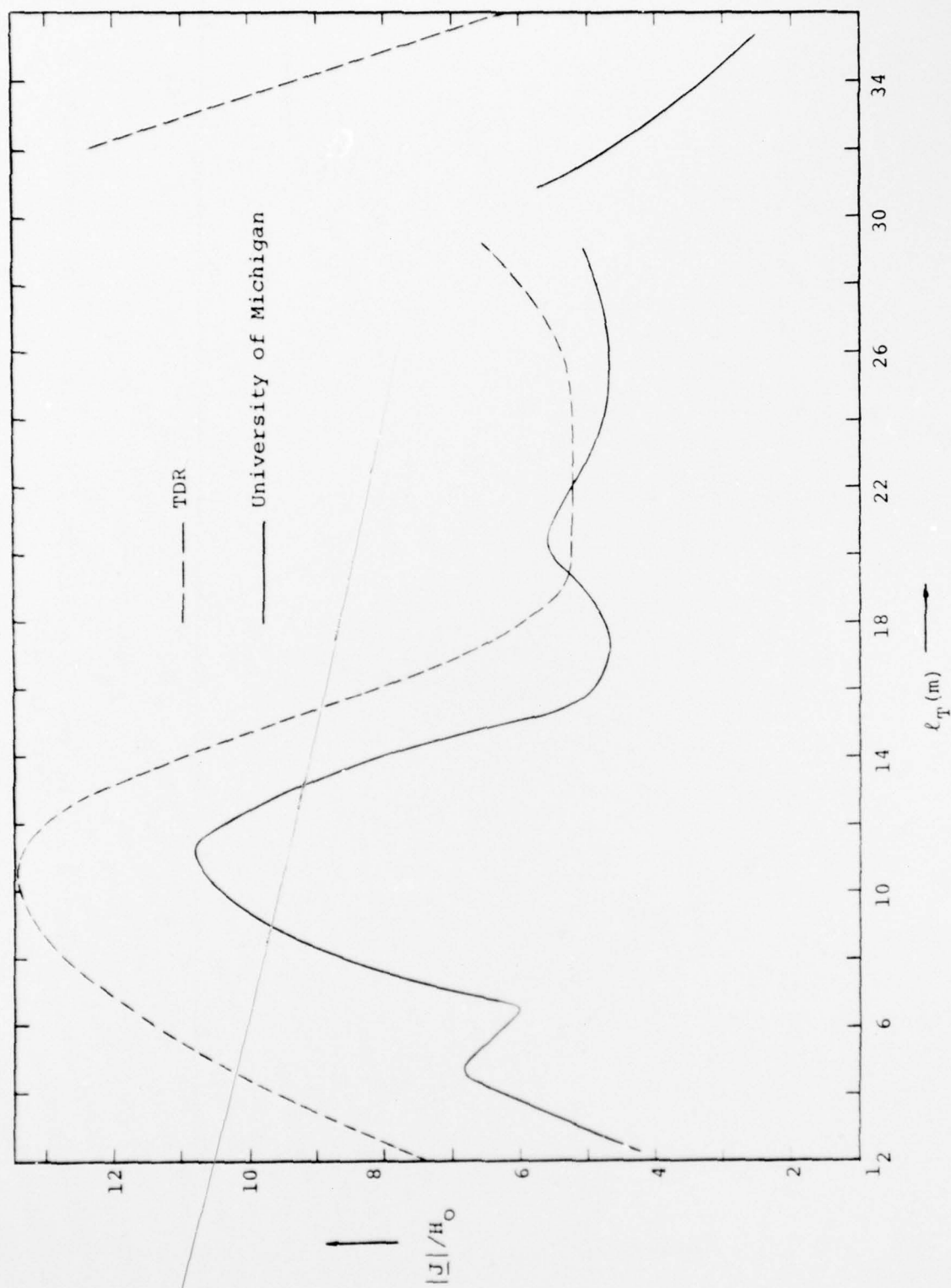Figure 14. Bottom of Fuselage, kh = 1.694. (h: Fuselage half length).

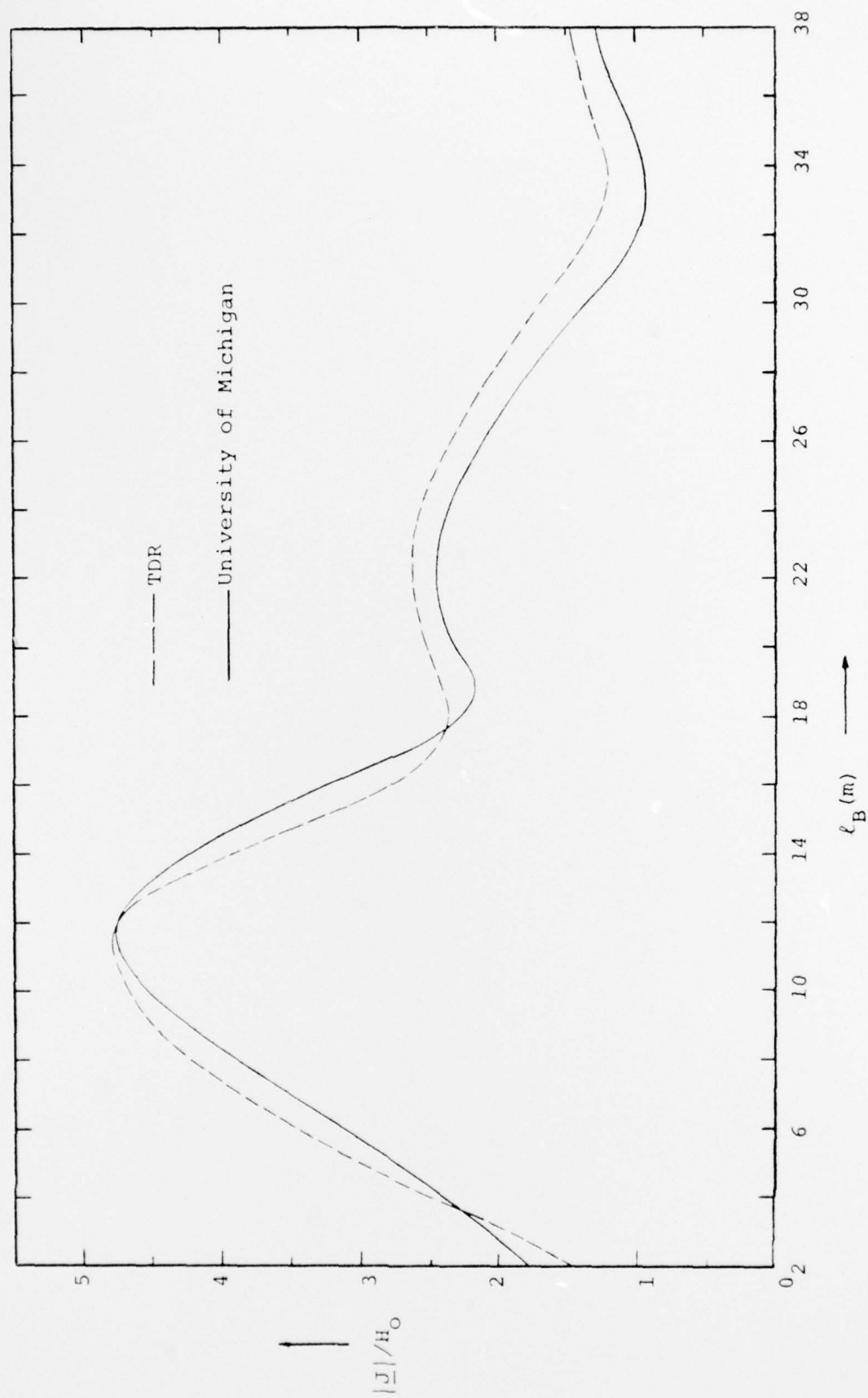Figure 15. Top of Fuselage, kh = 1.694. (h: Fuselage half length.)

Figure 16. Bottom of Fuselage, kh = 2.014. (h: Fuselage half length).

53
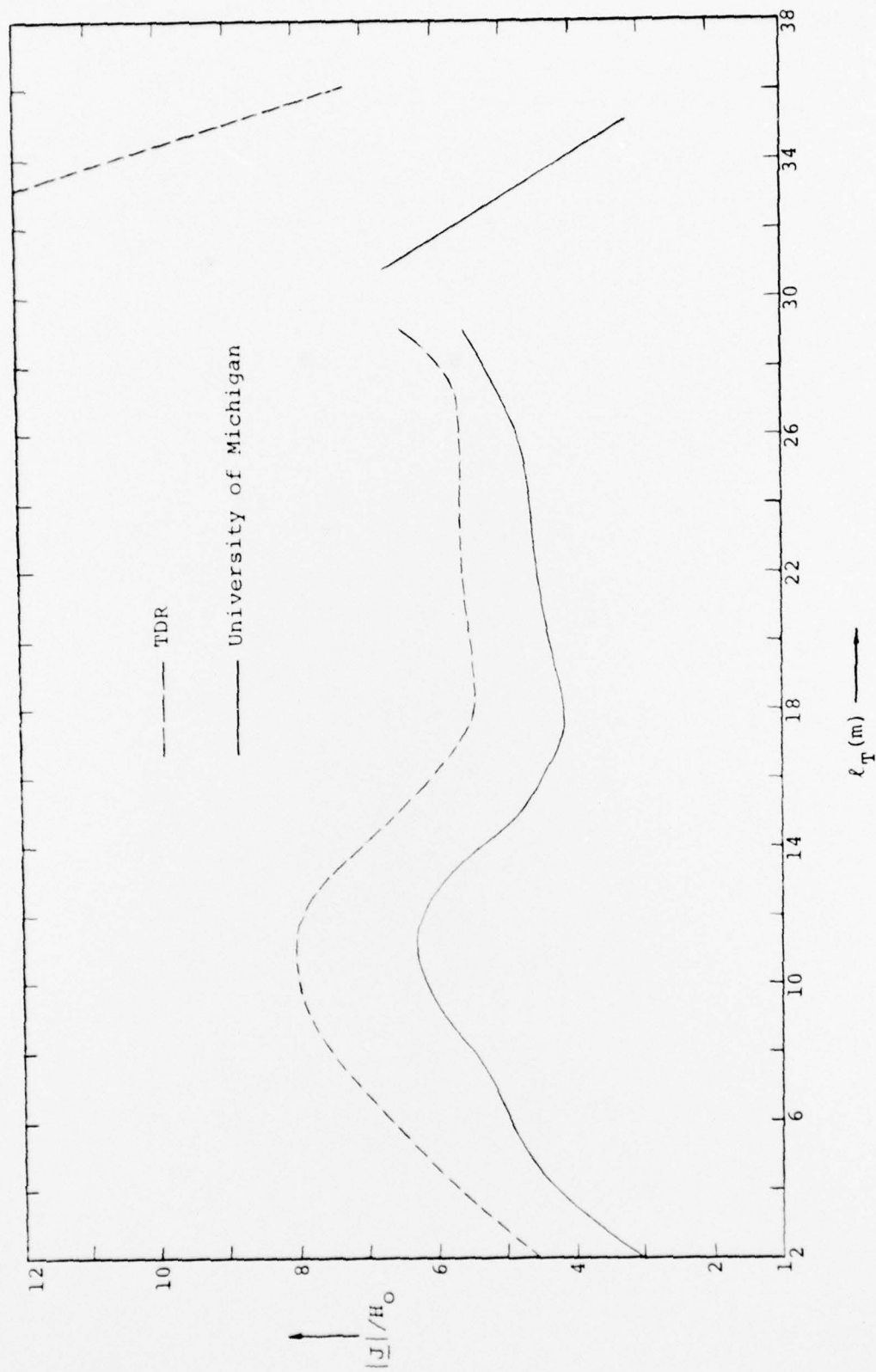
Figure 17. Top of Fuselage, kh = 2.014. (h: Fuselage half length.)

REFERENCES

1. Tai, C.T., Dyadic Green's Functions in Electromagnetic Theory, Intext Educational Publishers, Scranton, PA., 1971.

2. Tai, C.T., Eigen-Function Expansion of Dyadic Green's Functions, Mathematics Note 38, Air Force Weapons Laboratory, 1973.

3. Baños, A., Dipole Radiation in the Presence of a Conducting Half-Space, Pergamon, Oxford, 1966.

4. Lytle, R.J. and D.L. Lager, Numerical Evaluation of Sommerfeld Integrals, AFWL Mathematics Note 47, also Report No. UCRL-51688, Lawrence Livermore Lab., University of California, Livermore, CA. 94550, 1974.

5. Lager, D.L. and R.J. Lytle, Fortran Subroutines for the Numerical Evaluation of Sommerfeld Integrals Under Anderem, AFWL Mathematics Note 98, also Report No. UCRL-51821, Lawrence Livermore Lab., University of California, Livermore, CA. 94550, 1975.

6. Haddad, H.A. and D.C. Chang, Dyadic Green's Function for a Two-Layered Earth, Mathematics Note 50, AFWL-TR-77-69, Air Force Weapons Laboratory, February 1977.

7. Van Bladel, J., Electromagnetic Fields, McGraw-Hill, New York, 1964.

8. Lee, K.S.H., L. Marin, and J.P. Castillo, Limitations of Wire-Grid Modeling of a Closed Surface, Interaction Note 231, Air Force Weapons Laboratory, May 1975.

9. Sassman, R.W., The Current Induced on a Finite, Perfectly Conducting, Solid Cylinder in Free Space by an Electromagnetic Pulse, Interaction Note 11, Air Force Weapons Laboratory, 1967.

DISTRIBUTION LIST

No. Copies

DEPARTMENT OF DEFENSE

12   Defense Documentation Center
ATTN: DD

DEPARTMENT OF THE AIR FORCE

2   Air Force Weapons Laboratory
ATTN: SUL

1   Air Force Weapons Laboratory
ATTN: HO, Dr. Minge

1   Air Force Weapons Laboratory
ATTN: NT, Dr. Payton

2   Air Force Weapons Laboratory
ATTN: ELTE, Dr. Baum

1   Air Force Weapons Laboratory
ATTN: NT, J. Darrah

1   Air Force Weapons Laboratory
ATTN: ELT, Dr. Castillo

1   Air Force Weapons Laboratory
ATTN: ELTI, Dr. Chen

5   Air Force Weapons Laboratory
ATTN: ELTI, Capt Hudson

1   Air Force Weapons Laboratory
ATTN: ELTI, Mr. Prather

1   Air Force Weapons Laboratory
ATTN: DYC, Dr. Singaraju

1   Air Force Weapons Laboratory
ATTN: ELAT, Technical File

1   Air Force Systems Command
ATTN: DLWM

1   Air University Library
ATTN: LDE

1   PO's Official Record Copy

57/58